APRIL 2018 M.Sc. in Mechanical Engineering MUTHANA MRAWEH KHAIRI

UNIVERSITY OF GAZIANTEP

GRADUATE SCHOOL OF

NATURAL & APPLIED SCIENCES

THE EFFECT OF VARIABLE CROSS SECTIONAL TUBES ON THE PERFORMANCE OF FLAT PLATE SOLAR COLLECTORS

M.Sc. THESIS

IN

MECHANICAL ENGINEERING

BY

MUTHANA MRAWEH KHAIRI

APRIL 2018

The effect of variable cross sectional tubes on the performance of flat plate solar collectors

M.Sc. Thesis

in

Mechanical Engineering

University of Gaziantep

Supervisor

Prof. Dr. Mehmet Sait SÖYLEMEZ

by

Muthana Mraweh KHAIRI

April 2018

REPUBLIC OF TURKEY

UNIVERSITY OF GAZİANTEP

GRADUATE SCHOOL OF NATURAL & APPLIED SCIENCES

MECHANICAL ENGINEERING

Name of the thesis: The effect of variable cross sectional tubes on the performance of flat plate solar collectors

Name of the student: Muthana Mraweh KHAIRI

Exam date: 27.4.2018

Approval of the Graduate School of Natural and Applied Sciences.

Prof. Dr. A.Necmeddin YAZICI
Director

I certify that this thesis satisfies all the requirements as a thesis for the degree of Master of Science.

Prof. Dr. M. Sait SÖYLEMEZ
Head of Department

This is to certify that we have read this thesis and that in our consensus opinion; it is fully adequate, in scope and quality, as a thesis for the degree of Master of Science.

Prof. Dr. M. Sait SÖYLEMEZ
Supervisor

Examining Committee Members:	Signature
Prof. Dr. Kadir AYDIN	....
Prof. Dr. Recep YUMRUTAŞ	....
Prof.Dr. M. Sait SÖYLEMEZ	....

I hereby declare that all information in this document has been obtained and presented in accordance with academic rules and ethical conduct.

Muthana Mraweh KHAIRI

ABSTRACT

THE EFFECT OF VARIABLE CROSS SECTIONAL TUBES ON THE PERFORMANCE OF FLAT PLATE SOLAR COLLECTORS

KHAIRI, Muthana Mraweh

M.Sc. Thesis in Mechanical Engineering

Supervisor: Prof. Dr. M. Sait SÖYLEMEZ

April 2018

74 pages

Flat plate solar collectors are the heart of domestic solar water heating system, due to their permanent position, simple construction, low cost and require little maintenance. The major purpose of this work is to estimate numerically the performance of flat plate solar storage collectors and investigate the thermal enhancement by enhancement of dimensions and geometry. Five types of flat plate storage solar collectors were examined for Iraq-Baghdad climate conditions with tilt angle at 33.33^{o}. These types of collectors were flat plate solar storage collectors, which are trapezoidal, ellipsoidal, circular, square and triangle models. The analysis of these collectors is according to the absorption of solar radiation, heat loss from the collectors, temperature distribution of absorber and the working fluid flowing through the collectors. The collectors are simulated utilizing Matlab program. Comparisons between the calculated & measured results of outlet and inlet water temperatures was performed, it indicated a satisfactory agreement. Theoretical results show that highest outlet temperatures were 60.53 ˚C, 60.83 ˚C, 60.2 ˚C, 59.51 ˚C and 58.63 ˚C, at solar noon in the five models, respectively. Maximum values of efficiencies were calculated 57.2%, 56.48%, 56%, 55.52% and 54.53% in five models.

Key word: solar energy, flat plat collector, water heating system.

ÖZET

DEĞİŞKEN ÇAPRAZ KESİM TÜPLERİNİN DÜZ PLAKA GÜNEŞ KOLLEKTÖRLERİNİN PERFORMANSINA ETKİSİ

KHAIRI, Muthana Mraweh
Yüksek Lisans Tezi, , Makina Müh. Bölümü
Tez Yöneticisi: Prof. Dr. M. Sait SÖYLEMEZ

Nisan 2018
74 Sayfa

Düz plaka güneş kollektörleri, kalıcı konumlarına, basit yapılarına, düşük maliyetlerine ve az bakım gerektiren evsel güneş enerjili su ısıtma sisteminin kalbidir. Bu çalışmanın temel amacı, düz plaka güneş depolama kollektörlerinin performansını sayısal olarak hesaplamak ve boyut ve geometriyi geliştirerek termal iyileştirmeyi araştırmaktır. Irak-Bağdat iklim şartları için 33.33o eğim açısı ile beş tip düz plaka depolama güneş kollektörü incelenmiştir. Bu tip kolektörler, trapez, elipsoidal, dairesel, kare ve üçgen modelleri olan düz plaka güneş depolama kolektörleriydi. Bu kollektörlerin analizi, güneş ışınımının emilimine, kollektörlerden ısı kaybına, emicinin sıcaklık dağılımına ve kollektörlerden akan çalışma akışkanına bağlıdır. Kollektörler Matlab programı kullanılarak simüle edilmiştir. Çıkış ve giriş suyu sıcaklıklarının hesaplanan ve ölçülen sonuçları arasındaki karşılaştırmalar yapıldı, tatmin edici bir anlaşma belirtildi. Teorik sonuçlar, en yüksek çıkış sıcaklıklarının sırasıyla 60.83 ˚C, 60.53 ˚C, 60.2 ˚C, 59.51 ˚C ve 58.63 ˚C olduğunu göstermektedir. Maksimum verimlilik değerleri beş modelde 57.2%, 56.48%, 56%, 55.52% ve 54.53% olarak hesaplanmıştır.

Anahtar Kelimeler: güneş enerjisi, düz plaka toplayıcı, su ısıtma sistemi.

This thesis is dedicated to my father and mother.

ACKNOWLEDGEMENT

Primarily, I would like to thank the Allah for his guidance and rewards toward me and my family. Then, I would like to express my debt of the gratitude to **Prof. Dr. M. Sait SÖYLEMEZ** and **Prof. Dr. Recep YUMRUTAŞ** for their guidance, advice, criticism, encouragements, insight and suggestions throughout the research and preparation of this thesis.

Finally, I wish to express my special thanks to my family, my brothers, my sisters and friends in Iraq and Turkey, for their great encouragement throughout my work, and for their continual support and encouragement.

TABLE OF CONTENTS

Page

LIST OF TABLES

LIST OF FIGURES

CHAPTER 1

INTRODUCTION

1.1 Introduction

It is imperative for countries to acquire power from sources other than conventional fossil fuels. This is as a consequence of an increasing population, people becoming additional aware of environmental constraints, & the rising cost of conventional fuels. Nuclear and renewable energy sources will have to equip an increasing percentage of total power capacity. Nuclear power is still reliant on limited sources of fuel, and has strong environmental & political implications, limitations by which renewable energy is commonly unaffected. Therefore creates sense to deliberate renewable energy sources as a resources of power generation. The enormous supply of renewable energy is in the usage of solar energy [1]. Averages of solar radiation for Baghdad, capital of Iraq, described by (NASA 2008), are shown in Table 1.1 and annual insolation contour map of Iraq as shown Figure1.1 have established that practically all of Iraq has the potential areas for establishing large-scale solar utilities. The annual average of energy established daily from the sun ranges between 4.5 – 5.4 kWh/m^2 in Iraq. Because of auspicious climatic conditions & geographical location, in the most parts of Iraq receive very high solar insulation around 2000 kWh/m^2/year. To diminish the fossil fuel consumption it is therefore obligatory to go to the solar energy possibilities. Therefore, there is the probable to convert a percentage of that solar energy into heat & electricity energy. The flat plate collector reflected the economy & simplest means of collecting solar energy system application that necessitate thermal energy at low temperatures (< 100°C).

Table 1.1 monthly averaged insulation incident on a horizontal surface (kWh/m^2/day) in Baghdad [2].

Jan	Feb	Mar	Apr	May	Jun	Jul	Aug	Sep	Oct	Nov	Dec
2.96	4.03	4.98	5.39	6.48	7.56	7.00	6.71	5.55	3.98	2.98	2.62

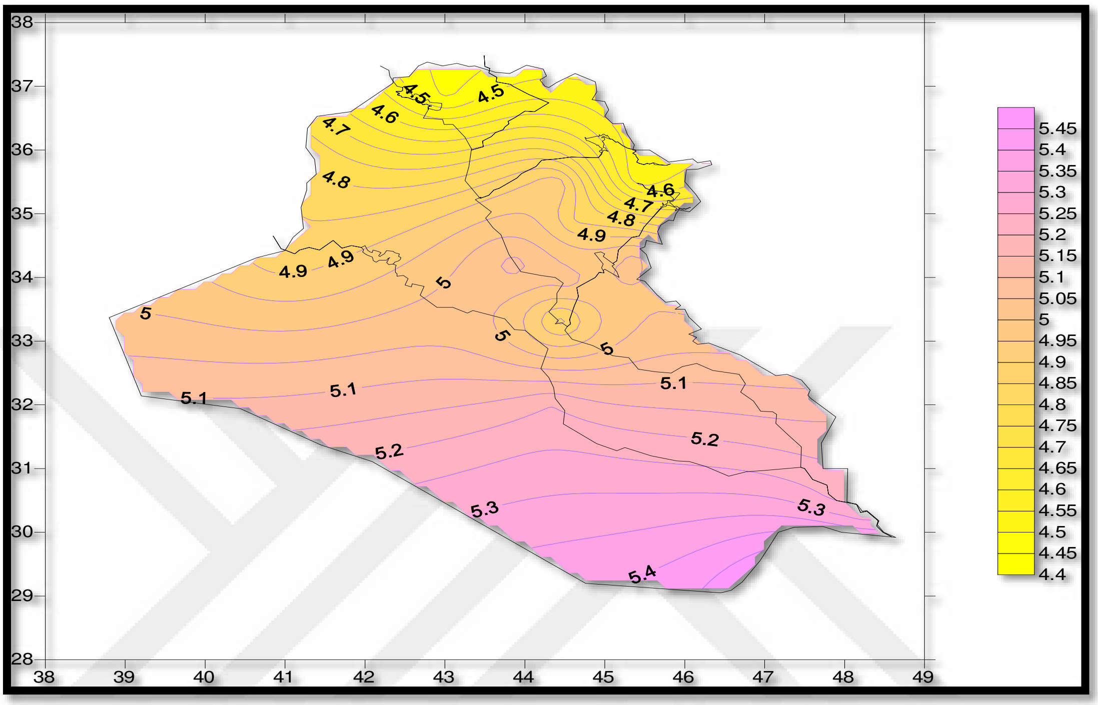

Figure 1.1 Daily-averaged solar insolation for different locations in Iraq [2]

1.2 Solar Collector

To transmute the solar energy into heat it is therefore obligatory to go to the solar collector which deliberate a special type of heat exchanger. Energy is transfer from a distant source of radiant energy to fluid in solar collector [3].There are various categories of solar collectors, ranging from air and liquid cooled, non-concentrating, flat plate collectors to multifaceted curvature, continuously tracking ones. Solar collectors are tabular mainly as active or passive. The aggregate of passive solar techniques, constructed on architectural design & building situation, with active systems can consequence in a highly operative energy conservation system. Passive solar collection incorporating the sun into the architecture of the building. The architect tries to capture two basic seasonal variations:

a) Cold weather, the destination is to maximize solar gain & maintain it in storage within the building.

b) Hot weather, the destination is to minimize solar gain into the building & dissipate it by forced or natural ventilation. These objectives are accomplished through proper utilization of the building structure’s external & internal components, including roof angle, & thermal insulation, as well as proper positioning of the building on site. Each element acting a valued role in reducing the building’s energy demand. Active solar collection techniques embrace flat plate collection, concentrating collection, & Photovoltaic (PV) collection. Each type possesses its own distinct advantages & disadvantages that must be reflected before it is preferred for a particular application [4].

1.2.1 Flat- Plate Solar Collectors

Flat plate collectors are very mutual & are obtainable for instance water-based collectors & liquid-based collectors. In low temperatures claims the flat plate collectors are superlative appropriate where the temperature between (30 - 70 °C) and/or for applications that oblige heat systems throughout the winter months. The liquid-based collector's application include regional heating & commercial hot water, building and interior swimming pools. A flat absorber collector resourcefully mutates solar energy (sunlight) into heat. To diminish heat losses in the collector supplement plate between insulating panel & glazing. The glazing is elected such that a maximum amount of sunlight will permit though it & influence the absorber. Figure 1.1.

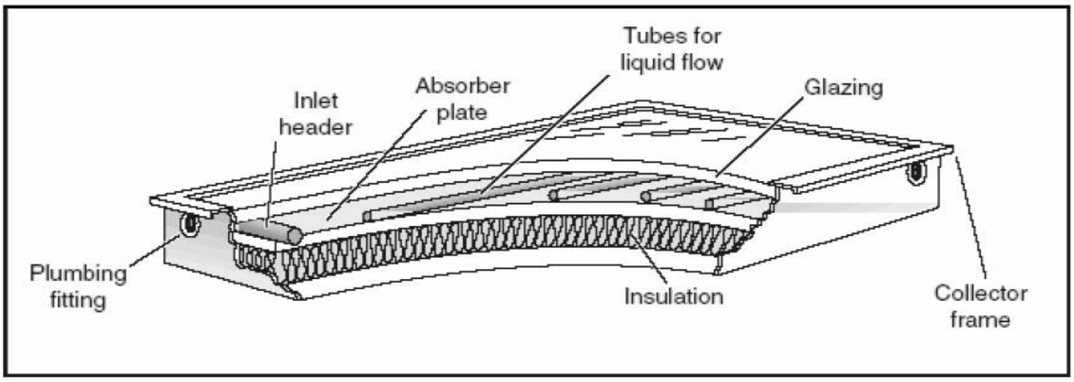

Figure 1.2 Flat plat solar collector [5].

1.2.2 Evacuated-Tube Solar Collectors

Evacuated-tube solar collectors contemplate the greatest resourcefully & costly that exceptional categories of solar collectors systems. The evacuated-tube collectors are superlative matched for restrained temperature applications where the temperature between (50-95°C) and/or for very cold climates. The vacuum tube collector's application consist of native heating & commercial hot water, building and interior swimming pools, like glazed flat plate solar collectors. Because of their aptitude to collect high temperatures resourcefully another potential application by refrigeration of reinforcing cycles for the buildings cooling. Solar collectors of evacuated-tube have a discerning absorber for collecting solar energy (sunlight) that characterized in vacuum-sealed tube. Evacuated-tube thermal losses are very low uniform in cold climates as shown in Figure 1.2.

Figure 1.3 Evacuated tube solar collector [5].

1.2.3 Concentrated Solar Collectors

By utilizing the reflectors the sunlight focused on the solar collector absorber then the size of absorber can be affectedly diminutive, at high temperatures which increases efficiency & diminishes heat losses as shown in Figure 1.3 [5]. This type of collector utilized in applications that necessitate high temperature such as thermal detoxification & steam production to generate the electricity. The focused collectors are better appropriate to climates that have a profusion of clear sky days. Stationary concentrating collectors may be air-based, liquid-based, or except a furnace such as a solar cooker.

Figure 1.4 Stationary concentrating solar collector [5].

1.3 Flat Plate Solar Collectors Used in the Present study

Three types of flat plate solar collector have been premeditated & assembled explicitly:

1. Solar collector with circular cross section channels.
2. Solar collector with square cross section channels.
3. Solar collector with triangle cross section channels.
4. Solar collector with ellipsoidal cross section channels.
5. Solar collector with trapezoidal cross section channels.

1.4 Objectives and Plane of the Present Study

The objective of the current labor is to estimate the advantages of utilizing five diameters models (square, trapezoidal, ellipsoidal, triangle and circular) inside the collector. The efficiency of five types of flat plate collectors is detected to predict the influence by utilizing three diameters models inside the collector (square, trapezoidal, ellipsoidal, triangle and circular).These objectives can be an accomplished by adopting the following plan:

1. Utilize the MATLAB software to generate a code that can numerically apply the proposed solution method.
2. Make enhancement by theoretical study for flat plate solar collector by using five diameters models inside the collector (square, trapezoidal, ellipsoidal, triangle and circular).
3. Making a comparison between the five models (square, trapezoidal, ellipsoidal, triangle and circular) of flat plate solar collector there are use it in this thesis to estimate the efficiency for each them.
4. Study the influence of various variables for three models (square, trapezoidal, ellipsoidal, triangle and circular) as geometry.
5. Study the influence size of diameter channels for five types of flat plate solar collectors (square, trapezoidal, ellipsoidal, triangle and circular).
6. The meteorological data was used for whole year (January to December) to accumulate the data obligatory to evaluate the performance of these collectors.
7. Completing all the numerical results to compare between them to validate this thesis.

CHAPTER 2
LITERATURE SURVEY

This chapter transacts with a historical literature review for the solar water heating system.

2.1 Solar Water Heating System

Hasan [6] simulated a thermo-syphone SWH exploiting the TRNSYS program. He checked the efficiency of heater by studying the hot water influence of storage tank volume and configuration. He indicated that a horizontal & vertical storage tanks determine comparable efficiencies.

Agbo [7] industrialized the design parameters of a thermo-syphone solar water heater utilizing MATLAB program. He simulated the influence of persistent water withdrawal rate on the mean system temperature of the heater under Nsukka environmental condition. The results indicated that as the mass withdrawal rate increases, the mean storage tank water temperature decreases, predicating on the time of the day.

2.1.1 Flat Plate Solar Collectors

The flat plate solar collector is regarded as the main part of any solar energy collection system designed for operating in the low temperature range or in the intermediate temperature range, the previous work on flat plate solar collectors can be ordered into:

2.1.1.1 Theoretical Studies

Shariah, et.al. [9] studied the influence of thermal conductivity of the absorber plate of a solar collector on the execution of a thermo-syphon solar water heater by the utilize of the transient simulation system (TRNSYS) software. The system was implicit to resource hot water at 55°C and 88°C representing both domestic and industrial uses respectively. Hot water of volumes 50, 125, and 250 liter is squandered daily according to the Rand apportionment profile. The results indicated that feature factors of the collector (specifically, heat removal factor, collector efficiency factor, and fin efficiency factor) and the annual solar fraction of the system have a so strong dependence on thermal conductivity of the absorber for its weak dependence and low values is observed a thermal conductivity amount beyond a value of (100 W/m°C −50W/m°C) for the feature factors and for the solar fraction respectively. the increased in the feature factors by about 12% and 19% and the annual solar fraction by about 4% and 7% because of an aluminum one is used instead of steel absorber plate whereas, the feature factors and the solar fraction are enhanced only by 3% and 1%, when a copper plate is used as a replacement for an aluminum one.

Zerrouki, et.al. [10] presented an analysis of natural circulation of a compact thermo-syphone solar domestic hot water (SDHW) system produced and commercialized locally in Algeria. Computations & mensuration were accomplished on the mass flow rate, temperature rise of fluid & absorber temperatures inside the thermo-syphone of parallel tube design.

Kundu and Lee [11] explored analytically of both Fourier & non-Fourier heat conduction in the absorber plates of a flat-plate solar collector. The variables separation was engaged to accomplish the temperature distribution. For the analysis, by solution of hyperbolic & parabolic equations utilize a repetitive heat transfer module. Firstly utilize separately two kinds of boundary conditions. For determination the temperature to authorize dedications according to the finite difference method was employed a numerical technique used. For understanding the requirements for use of the non Fourier heat conduction model easily making a comparative investigation. A presumed difference in the temperatures obtained from the no Fourier & Fourier models was detected for lower amounts of the Fourier number & higher values of the Vernottee number, which is defined as:

$$V_e = \frac{\sqrt{\tau\alpha}}{L_1} \qquad (2.1)$$

τ = is thermal relaxation time

α = thermal diffusivity

L_l = length of absorber

Kalogirou [12] investigated through modeling and simulation the effect of configuration parameters with enhance the execution of the natural circulation solar water heater. These considerations titled number of the distance between the top of collector to the bottom side of the storage tank, risers, header diameter, and the collector incline. The better system is obtained for small header & riser pipe diameters. The most favorable collector tilt angle is established to be identical to the latitude plus 10˚, and the optimum distance between the top of collector and the bottom of the storage tank (- 15 cm).

2.1.1.2 Experimental Studies

Abd-Alzahra and Joudi [13] examined a forced circulation solar water heater to assess its performance under several operating conditions. The system contained of two homogeneous collectors of total absorber area of 3.45 m^2 and a storage tank of 200 liter capacity. Experiments were carried out during clear days with and without system loading for two water mass flow rates through the collector; namely 7.83l/min and 3.915l/min. The system was operated without thermostat control & with thermostat control at maximum & minimum settings. The collector efficiency improved with system loading. The enhancement was better with increased hot water withdrawal from the system. They also investigated experimentally the thermosyphone solar water heater in 1984. The system comprised of a flat-plate collector of 1.5 m^2 absorber area with 21 tubes/m width & storage tank of 125 liters capacity. Experiments were carried out for both cloudy & clear weather conditions in winter & summer. They evaluated the hourly system performance for all test conditions. The final mean tank temperature was measured daily which enabled the calculation of the possible contribution of solar energy for domestic hot water supply in Basra, Iraq (latitude 30.76°N). They experimented the system at both no load & loading conditions. Intermittent & continuous load was executed, and system performance was evaluated for each condition.

Sekhar et.al. [14] deduce top loss coefficient of flat plate collector both theoretically & practically. Under the conditions of laboratory a test setup is fabricated and experiments conducted to study these aspects. The analysis of Theoretical & practical is performed on a flat plate collector with a single glass cover. It could be accomplished that the emissivity of the absorber plate has a substantial impact on the top loss coefficient & consequently on efficiency. By increasing ambient temperature the efficiency increased. Without presumed impact of tilt angle on the top loss coefficient.

Hobbi and Siddiqui [15] explored practically the impact of heat enhancement devices on the thermal performance of a flat-plate solar collector such as twisted strips, coil-spring wire & conical ridges. The comparison showed no ratable difference in the heat flux to the collector fluid for the different enhancement devices. An elaborate examination of the utilized trend indicated considerably high values of Grashoof, Richardson & Rayleigh numbers indicating that the heat transfer mode in the solar collector is of contented convection type & free convection as the established mode. They concluded that due to the substantial damping of shear & produced turbulence by buoyancy forces, the applied passive methods based on the enhancement of shear-produced turbulence are ineffectual in increasing heat transfer to the collector fluid in flat-plate solar collectors.

Sutthivirode et.al. [16] enhanced the thermal efficiency of a solar water heating system (SWHS) coupled with a built-in solar water pump by elimination of the heat losses from the storage tank. The considered system contains of 1.58m^2 flat plate solar collectors, an overhead tank positioned at the top level, the larger water storage tank without a heat exchanger at the lesser level, & a one-way valve for water circulation control. Recognized the discharge heads of 1 and 2 m. The pump could engage at the collector temperature of about 70-90 ℃ & vapor gage pressure of 10-18 kPa. It was set up that water circulation within the SWHS ranged between 15 and 65 Liter/day depending upon solar intensity & discharge head. Over & above the max water temperature in the storage tank is around 59 ℃. The max daily pump efficiency is about 0.0017%. The solar water heating system reproduce max daily thermal efficiency reach to 21%. It is consummated that the thermal efficiency was successfully enhanced, not including the pump.

Jaisankar, et.al. [17] investigated practically heat transfer & friction factor characteristics of thermo-syphone solar water heater system with tube collector inserted with full- length, twist tape with rod & spacer fitted at the trailing edge for lengths of 100, 200 and 300 mm with twist ratio of 3 and 5. They compared it with ordinary tube collector for the itself operating conditions. The experimental data for Nusselet number & friction factor for ordinary tube collector is verified with fundamental equations. They industrialized empirical correlations for Nusselet number & friction factor for twist ratio 3 and 5. Their enhancement indicate that the decrease in Nusselet number for full length helical twist paralleled to twisted tape with rod is minimum and is quite significant for twist with spacer. But the rebate in friction factor is maximum in twist be suitable for the spacer paralleled to twisted tape with rod. The overall execution for twisted tape with rod is implement to be better than twist be suitable for the spacer.

Huang, et.al. [18] explored practically the thermal performance of thermo-syphone flat-plate solar water heater with a mantle heat exchanger to appearance its applicability in China. They analyzed the execution of the collector using an exchanger between the collector and the tank. A heat exchanger retribution factor for heat the system was determined and energy balance equation in the system was presented. outcomes indicate that mean daily efficiency of the thermo-syphone flat plate solar water heater with a mantle heat exchanger with 10 mm gap can reach up to 50%, which is worse than that of a thermo-syphone flat-plate solar water heater without heat exchanger, but upper than that of an all-glass evacuated tubular solar water heater.

Tang, et.al. [19] studied the influences of water temperature in the storage tank & height modification between the storage tank and the collector on freeze shield of flat-plate collectors at clear nights in standings of outlet water temperature of the thermo-syphone reverse flow from the collector (referred to as T_{out}). They reported that higher outlet water temperature T_{out} was obtained from tank in vertical orientation rather than that in horizontal orientation. They deduced that T_{out} increased with the increase of water temperature in the tank but was lower than the ambient air temperature all night. They also scrutinized a mathematical model and experimentally validated for the execution parameters of the system on T_{out} at clear nights. This prototypical permits prophesy Tout & the time at the moment of ice formation inside absorber of the collector begins. Arithmetical results deduce that the collector-tank height modification & the thermal emissivity of absorbers have substantial influence on the freeze shield of collectors in standings of T_{out}; for the system with a collector of non-selective absorber, the anticipated T_{out} was lower than the ambient air temperature, as detected in experiments; forasmuch for the system with a collector of solar selective absorber, the T_{out}, depending on water temperature in the storage tank, was higher than the ambient air temperature. This outcome implied that, in thermo-syphone Solar regional Water System, flat-plate collectors with a non-solar-selective absorber might suffer from freezing-damage, but those with a solar selective absorber would not, at clear nights with ambient air temperature thereabouts & except lower than the freezing temperature.

2.1.1.3 Porous Media and Solar Collectors

Hassab et al. [20] examined a flat plate solar air collector in which air flows perpendicularly from the translucent cover to the porous absorber plate. This collector is premeditated such that no natural convective invasions take place under various system parameters. The results signalize that the best operating efficiency can be achieved when running the collector with a mass flow rate of m >40 kg/m.h.

Chen and Liu [21] considered numerically heat transfer and air flow in an amalgamated wall solar collector system with a porous absorber. They used this collector as a thermal insulator when sunlight is not available and as an air header during day. The effect of particle size and the porous layer thickness on the air temperature inside the heater room have been investigated. They found the space temperature reaches 27 ˚C for wall porosity of 0.25 % when the out side average temperature was 10 ˚C and maximum solar radiation was 350 W/m^2.

Yousef [22] studied theoretically the influence of mass flow rate, flow channel depth and collector length on the system thermal execution and pressure drop through the collector with and without porous medium. The solution transaction is unequivocal for flat plate collector in single and double flow mode. The results deduce that the system thermal efficiency increases by 10-12% in double flow mode than single flow due to the increased of heat removal, and increases by 8% after using porous medium in the lower channel as a result of the increase of heat transfer area. Itself time the pressure drop will be increased.

Chen and Huang [23] presented a numerical study of enhanced forced convection in a channel of solar water collector using discrete metal foam blocks. They adopted both Darcy- Brinckman- Forchheimar flow model and two equation energy model based on local non- equilibrium, to evaluate the thermo fluid fields inside the porous regions. In the fluid region they used Navier & Stokes equation. Their results deduce that an improvement in flat plate thermal execution is obtained by inserting the porous blocks. However an increase in pressure drop is reported according to the size material and properties of metal foam blocks.

2.2 Scope of the Present Study

Many of literatures in the field of flat plate collector with and without optimization of diameters and geometry were done during the last few decades. Most of the review works studied flat plate collector without optimization of diameters and geometry and few of researchers investigate the effect of diameters optimization on flat plate solar collectors.

The novelty of this work is to scrutinize the inserted five types of channels in flat plate solar collector. The contribution of the present work can be expressed as:

1. Using a new type of collector system by enhancement the diameters and geometry.

2. Investigate the wavy channels in this collector by using five type of channels for multi zones domain.

3. Developing the mathematical model of the adopted design with the appropriate boundary conditions and interface condition.

4. Specify the effect of utilizing this new type of collector on the thermal execution of solar water heating system for Iraq limit conditions.

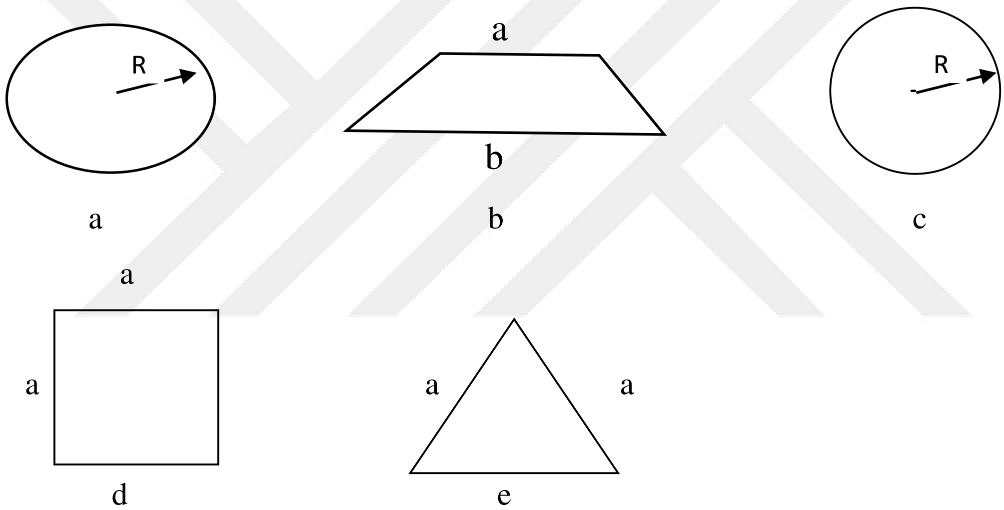

Figure 2.1 Cross-sections of five types of pipes inside collector, (a) ellipsoidal pipe (b) trapezoidal pipe (c) circular pipe, (d) square pipe and (e) triangle pipe.

CHAPTER 3

THEORETICAL STUDY

This chapter includes the theoretical foundation in the calculation of the amount of absorption and loss energy. Also included how to calculate the overall heat loss coefficient and calculate the useful and storage energy. Efficiency of the solar collector with heat storage efficiency were calculated. Finally, mathematical model was developed to calculate all the variables in this chapter. As well as a computer program has been developed. A steady state assumption is used in calculations.

3.1 Data analysis method

The following simplified steps were used to analyze the heat transfer for the water flow across the channels and to calculate the amount of energies and the efficiency.

3.2 Absorption energy calculation

The absorption energy could be calculated by the equation below:

$$Q_{ab} = F_t \, I_t \, A \tag{3.1}$$

Where, I_t is the total incident radiation. The effective transmittance-absorption factor F_t is calculated from the following equation:

$$F_t = (\alpha_p \tau_g)_e \, F_{sh} \, F_d \tag{3.2}$$

$(\alpha_p \tau_g)_e$ is calculated as follows:

$$(\alpha_p \tau_g)_e = 1.02 \, \alpha_p \tau_g \tag{3.3}$$

3.3 Energy loss calculation

Energy losing is happening from all sides of the solar collector, in spite of the biggest part of losing is from the absorber surface. However, losing energy from sides and bottom has a clear effect.

The amount of energy losing is given by the following equation:

$$Q_{loss} = U_l\, A\, (T_p - T_a) \tag{3.4}$$

Mean plate temperature (T_p) is calculated as follows:

$$T_p = T_i + \frac{Q_u/A}{F_R U_l}\,(1 - F_R) \tag{3.5}$$

The heat removal factor F_R is given as:

$$F_R = F''F' \tag{3.6}$$

Where the collector flow factor F'' and the collector efficiency factor F' are calculated as follows:

$$F'' = \frac{\dot{m}_w\, c_p}{AU_l F'}\left[1 - \exp\left(-\frac{AU_l F'}{\dot{m}_w\, c_p}\right)\right] \tag{3.7}$$

$$F' = \left[\frac{1/U_l}{W\left(\frac{1}{Ul[D+(W-D)F} + \frac{1}{\pi D h_f}\right)}\right] \tag{3.8}$$

$$F = \frac{\tanh m(W-D)/2}{m(W-D)/2} \tag{3.9}$$

$$(m)^2 = \left(\frac{Ul}{k\delta}\right) \tag{3.10}$$

The collector overall heat transfer coefficient (U_l) is the sum of top, bottom and edge loss coefficients:

$$U_l = U_t + U_b + U_e \tag{3.11}$$

The bottom loss coefficient is found from equation bellow:

$$U_b = \frac{K_b}{X_b} \tag{3.12}$$

The edge loss coefficient based on the collector area is found as follows

$$U_e = \frac{K_e}{X_e} \frac{A_e}{A} \tag{3.13}$$

The top loss coefficient from the collector plate to the ambient for this single glass cover system is as follows:

$$U_t = \left[\frac{1}{h_{c,p-g}+h_{r,p-g}} + \frac{1}{h_w+h_{r,g-a}} \right]^{-1} \tag{3-14}$$

The wind heat transfer coefficient is calculated as:

$$h_w = 5.7 + 3.8\ v \tag{3.15}$$

The radiation heat transfer coefficient from the glass to the ambient ($h_{r,g-a}$) is calculated as:

$$h_{r,g-a} = \varepsilon_g \sigma \left(T_g + T_s\right)\left(T_g^2 + T_s^2\right) \tag{3.16}$$

The radiation heat transfer coefficient from the plate to the glass cover ($h_{r,p-g}$) is calculated as:

$$h_{r,p-g} = \frac{\sigma\left(T_p+T_g\right)\left(T_p^2+T_g^2\right)}{\frac{1}{\varepsilon_p}+\frac{1}{\varepsilon_g}-1} \tag{3.17}$$

3.4 Tubes models

There are five geometries models for pipe of the solar collectors, which are:

3.4.1 Trapezoidal model

In the case with trapezoidal channels D_h is given by:

$$D_h = 1.054\ D \tag{3.18}$$

3.4.2 Ellipsoidal model

In the case with ellipsoidal channels D_h is given by:

$$D_h = 0.89\ D \quad (3.19)$$

3.4.3 Circular model

In the case with circular channels D_h is given by:

$$D_h = D \quad (3.20)$$

Where D is diameter of the channel.

3.4.4 Square model

In the case with square channels D_h is given by:

$$D_h = 0.886\ D \quad (3.21)$$

3.4.5 Triangle model

In the case with triangle channels D_h is given by:

$$D_h = 0.773\ D \quad (3\text{-}22)$$

The useful gain of the solar collector is calculated as follow:

$$Q_u = F_R A[S - U_l(T_i - T_a)] \quad (3.23)$$

Which is also can be calculated as:

$$Q_u = \dot{m}_w\ c_p\ (T_o - T_i) \quad (3.24)$$

From equation (3-24) the outlet temperature is:

$$T_o = T_i + Q_u/\dot{m}_w\ c_p \quad (3.25)$$

Q_u in equation (3-24) is found from equation (3-25).

3.5 Thermal efficiency calculation

The efficiency of the flat-plate solar collector (η_c) is define as the ratio of the rate of useful energy supplied by the collector (Q_u) to the rate of incident solar energy in its area.

$$\eta_c = \frac{Q_u}{Q_I} \tag{3.26}$$

The incident solar energy on the solar collector area is found by multiplying the total solar intensity (which is found meteorological data) by the collector area.

$$Q_I = I_t A \tag{3.27}$$

CHAPTER 4

ANNUAL FRACTION LOAD ANALYSIS

4.1 Introduction

The analysis in this chapter about the monthly and the annual performance of a solar water heating system for the trapezoidal, ellipsoidal and circular flat plate solar collector (FPSC). These types of the collector were the optimum that obtained in the study for five models of collectors the selecting the optimum design depend on the fraction load calculations that will be completed in this chapter. Finally the fraction load calculation is very important to object the enhancement of the flat plate solar storage collector.

4.2 Annual Fraction load by Solar Energy Analysis

the objective of this analyses to estimate the annual and monthly load for flat plate solar collector that use for service water heating system after that we can select the optimum design based on the annual fraction thermal performance. The equation of the fraction load (F):

$$F = \Sigma f \; Li / \Sigma Li \qquad (4.1)$$

4.2.1 The f-Chart Method

The outline the f-chart method for estimating the annual thermal performance of active heating systems for the building that using the liquid or the air as a working fluid the f-chart method provides a means for estimating the fraction of annual heating load that will be supplied by the solar energy for heating system then the primary design variable is a collector area the secondary variable is a collector type, storage capacity, fluid flow and the load. The f-chart for the liquid systems as a function for X and Y:

$$f = 1.029\, Y - 0.065\, X - 0.245\, Y^2 + 0.0018\, X^2 + 0.0215\, Y^3 \quad (4.2)$$

The load in the f-chart method include the energy requirement for heating of hot water

$$L = Cp\ M\,(Tw - Tm) \quad (4.3)$$

4.3.2 Service Water Heating System

The f-chart method for liquid heating system can be used to estimate the performance of solar water heating system by defining an additional correction factor on X. The supply water temperature and the hot water temperature both effect on the performance of solar water heating system, also effect on the average system operating temperature level and energy losses. The dimensionless group X, which is related to collector energy losses can be corrected to include these effects. Then the two dimensionless group are:

$$X = X\,(Xc / X) = Ac\ FR\ Ul.(11.6 + 1.8\ Tw + 3.86\ Tm - 2.32\ Ta)\ at/L \quad (4.4)$$

$$Y = Ac\ FR(ta)\ I\ N/L \quad (4.5)$$

CHAPTER 5

SOLAR ECONOMICAL ANALYSIS

5.1 Introduction

The objective of this chapter to calculate the monthly and the annual performance of a solar water heating system and the economics of the solar collector the solar processes are generally characterized by high first cost and low operating cost then the solar energy equipment bought today to reduce tomorrows fuel bill.

5.2 Solar Economics Analysis

The objective of the economics analysis can be viewed as the determination of least cost method of meeting the energy need considering solar or non-solar alternative. For the solar energy processes, the problem is to determine the size of solar energy system that give the lowest cost combination of the solar and auxiliary energy. In this chapter we outline the life cycle savings method of doing economics analyses. This method take into account the time value of money and allow detailed consideration of complete range of costs.

5.2.1 The cost of solar process systems

The investments in buying and installing solar energy equipment are important factors in solar process economics. These include the delivered price of equipment such as collectors, storage unit, pumps and blowers, control, pipes and ducts, heat exchanger and all the other equipment must also be associated with the solar installation.

The installed cost of the solar equipment can be shown as the sum of two terms, the proportional to the collector area and the other independent collector area:

$$C_S=C_A A_C+C_E \quad (5.1)$$

Where C_S= total cost of installed solar energy equipment. ($)

C_A=total area dependent costs, ($/m^2)

A_C=collector area. (m^2)

C_E=the cost of equipment which is independent of collector area. ($)

The area dependent the costs, C_A, include such items as the purchase and the installation of the collector and a portion of storage costs. The area independent the cost, C_E, include such items as controls and bringing construction or erection equipment to the site which do not depend on collector area.

5.2.2 Life cycle savings method

The objective of calculate the life cycle solar savings to find the collector size that combination of the solar energy and which provides the highest savings. Now we apply the ideas in this study to illustrate the principles and steps in the life saving analyses the select the optimum design will be based on the solar saving calculation for several collector areas. The simple formulation for life cycle savings (LCS):

$$LCS=P1\ C_{F1}\ L\ F-P2\ (C_A A_C+C_E) \quad (5.2)$$

Where C_{F1}=the first fuel cost ($/GJ)

L=annual load (GJ)

F=fraction load by solar energy.

P1=is the ratio of the life cycle fuel cost saving to the first year fuel cost savings.

P2=is the ratio of the life cycle expenditures incurred because of the additional

Capital investment to the initial investment

C_A=total area dependent costs, ($/m^2)

$A_{C=}$collector area. (m^2)

C_E=the cost of equipment which is independent of collector area. ($)

The derivative of the savings with respect to the collector reach zero:

$$d(LCS)/dA=0= P1\ C_{F1}\ L\ dF/dA- P2\ C_A \quad (5.3)$$

The maximum savings are realized when the relationship between the collector area and the solar load fraction satisfies:

$$dF/dA=P2\ C_A/P1\ C_{F1}\ L \quad (5.4)$$

The relationship of the optimum area to the annual thermal performance will be calculated then the optimum area occurs where the slope of the curve is P2 C_A/P1 C_{F1} L.

CHAPTER 6

RESULTS AND DISCUSSIONS

6.1 Introduction

This chapter describes and discus theoretical results of flat plate solar collector and validate the model written by MATLAB program to obtain the optimum design and type collector.

In this study, the five types of flat plat solar collector are studied hour by hour from January to December then the objective of this study to select the optimum model after completed this study on the five types of collector square, trapezoidal, ellipsoidal, triangle and circular we obtain the trapezoidal, ellipsoidal and circular collectors were optimum. The efficiency, the outlet temperatures of hot water, heat removal factor, useful gain energy, and overall heat loss coefficient had been calculated for the square, trapezoidal, ellipsoidal, triangle and circular models. The hourly outlet water temperature for five models of collectors which were square, trapezoidal, ellipsoidal, triangle and circular from January to December obtained. The temperatures values along the solar collector represented in these study in five models. The Maximum values of outlet water temperatures were at solar noon in five models trapezoidal, ellipsoidal, circular, square and triangle we noticed that the temperature increase from sunrise time and reach to the maximum at noon time and it decreases gradually until it reach to minimum value at sunset time . The monthly and annually load, fraction load by solar energy for several areas and mass flow rate, f-chart, f-calculation hour by hour, monthly and annually and life cycle savings for several areas and mass flow rate had been calculated. The results, which were obtained from the study of five types of flat plate solar collectors are calculated for whole year. The hourly values of solar radiation, the hourly values of ambient temperatures and hourly values of the wind speed are taken from Iraqi Meteorological Organization and Seismology Fraction load by solar energy and the monthly load and annually load for the flat plate solar collector during the period from January to December then annual heating load was obtained. The results of the heating load calculation, were used as input parameters in order to obtain the calculation of economical analysis. The economical analysis was based on the life cycle solar savings analysis. Finally, the life cycle savings for collector were obtained.

6.2 Computational procedure for the FPSC

The purpose of this section is to represent the computation procedure of all of numerical calculations explained in chapters 3, 4 and 5. A computer program was prepared in Matlab in order to carry out all the numerical calculations which are the calculations of the efficiency, the outlet temperatures of hot water, heat removal factor, useful gain energy, and overall heat loss coefficient for five models. The monthly and annually load, fraction load by solar energy for several areas and mass flow rate, f-chart, f-calculation hour by hour, monthly and annually and life cycle savings for several areas and mass flow rate for the circular collector. The results, which were obtained from the study of five types of flat plate solar collectors are calculated for whole year. In this study, the five types of flat plat solar collector are studied hour by hour from January to December then the objective of this study to select the optimum model after completed this study on the five types of collectors we obtain the trapezoidal, ellipsoidal and circular collector were optimum.

6.2.1 Computational procedure for theoretical analysis

A computational program is prepared in MATLAB to perform the numerical computations based on developed analytical model. This section includes the theoretical foundation in the calculation of the amount of absorption and loss energy. Also included how to calculate the overall heat loss coefficient and calculate the useful and storage energy. Efficiency of the solar collector with heat storage efficiency were calculated. Finally, mathematical model was developed to calculate all the variables in this study. As well as a computer program has been developed. A steady state assumption is used in calculations. The MATLAB program uses several parameters, which are type of the collector, the hourly solar radiation data, ambient temperature data and wind speed data used as input data for the program.

6.2.2 Computational procedure for fraction load by solar energy

The purpose of this part is to represent the computation procedure of fraction load by solar energy calculation which represent in chapter 4. the objective of this analyses to estimate the annual and monthly load for flat plate solar collector that use for service water heating system after that we can select the optimum design based on the annual fraction thermal performance was calculated using Equation (4.1). The f-chart method for liquid heating system can be used to estimate the performance of solar water heating system by defining an additional correction factor on X. The supply water temperature and the hot water temperature both effect on the performance of solar water heating system, also effect on the average system operating temperature level and energy losses. The dimensionless group X, which is related to collector energy losses can be corrected to include these effects were obtained by using equation (4.3).

6.2.3 Computational procedure for economical analysis

The purpose of this part is to represent the computation procedure of economic calculation which represent in chapter 5. The solution of the economical analysis was carried out by using the life cycle savings analysis. The objective of the economics analysis can be viewed as the determination of least cost method of meeting the energy need considering solar or non-solar alternative. For the solar energy processes, the problem is to determine the size of solar energy system that give the lowest cost combination of the solar and auxiliary energy. In this chapter we outline the life cycle savings method of doing economics analyses which was calculated using equation (5.1). The objective of calculate the life cycle solar savings to find the collector size that combination of the solar energy and which provides the highest savings. Now we apply the ideas in this study to illustrate the principles and steps in the life saving analyses the select the optimum design will be based on the solar saving calculation for several collector areas which was calculated using equation (5.2).

6.3 Results for Solar Hot Water System

The study of the thermal performance of the flat plate solar collector integrated with the new designed trapezoidal, ellipsoidal, square and triangle models are calculated for whole year.

6.3.1 Measured Results

The calculation was completed during the period from January to December in Iraq-Baghdad. The collector tilt angle was 33.33˚ degrees. The readings were used from sunrise to sunset.

6.3.2 The temperature calculation for the Solar Collector

A thermo syphone flat plate solar collector has been tested from the sunrise to the sunset for clear sky. The temperatures of water outlet, absorber plate, glazing cover of the collector were calculated for whole year. The useful heat gain, the storage energy, the efficiency of the collector and the energy of loss were calculated according to these measurements. The Maximum values of outlet water temperatures were at solar noon in five models we noticed that the temperature increase from sunrise time and reach to the maximum at noon time and it decreases gradually until it reach to minimum value at sunset time . Figures (6.1), (6.2), (6.3), (6.4), (6.5), (6.6), (6.7), (6.8), (6.9), (6.10), (6.11), and (6.12) show the Variation of outlet water temperature with time for three models of collectors which were circular, square and triangle for whole year.

Figure 6.1 shows that the maximum temperature of outlet water was 51.09 °C in circular model, 50.24°C in square model and 49.08°C in triangle model on January. Figure 6.2 shows that the maximum temperature was 58.72°C in circular model, 57.87°C in square model and 56.69°C in triangle model on February. Figure 6.3 shows that the maximum temperature was 59.74°C in circular model, 58.89°C in square model and 57.71°C in triangle model on March. Figure 6.4 shows that the maximum temperature was 62.40°C in circular model, 61.42°C in square model and 60.78°C in triangle model on April. Figure 6.5 shows that the maximum temperature was 59.59°C in circular model, 58.44°C in square model and 57.22°C in triangle model on May. Figure 6.6 shows that the maximum temperature was 58.88°C in circular model, 57.72°C in square model and 56.50°C in triangle model on June. Figure 6.7 shows that the maximum temperature was 59.93°C in circular model, 58.79°C in square model and 57.56°C in triangle model on July. Figure 6.8 shows that the maximum temperature was 56.92°C in circular model, 56.07°C in square model and 55.02°C in triangle model on August. Figure 6.9 shows that the maximum temperature was 53.10°C in circular model, 52.25°C in square model and 51.18°C in triangle model on September. Figure 6.10 shows that the maximum temperature was 50.75°C in circular model, 49.90°C in square model and 48.83°C in triangle model on October. Figure 6.11 shows that the maximum temperature was 52.60°C in circular model, 51.74°C in square model and 50.59°C in triangle model on November. Figure 6.12 shows that the maximum temperature was 49.31°C in circular model, 48.45°C in square model and 47.31°C in triangle model on December. Then the difference between the temperatures of the three types because the difference in the surface area which be under the solar intensity.

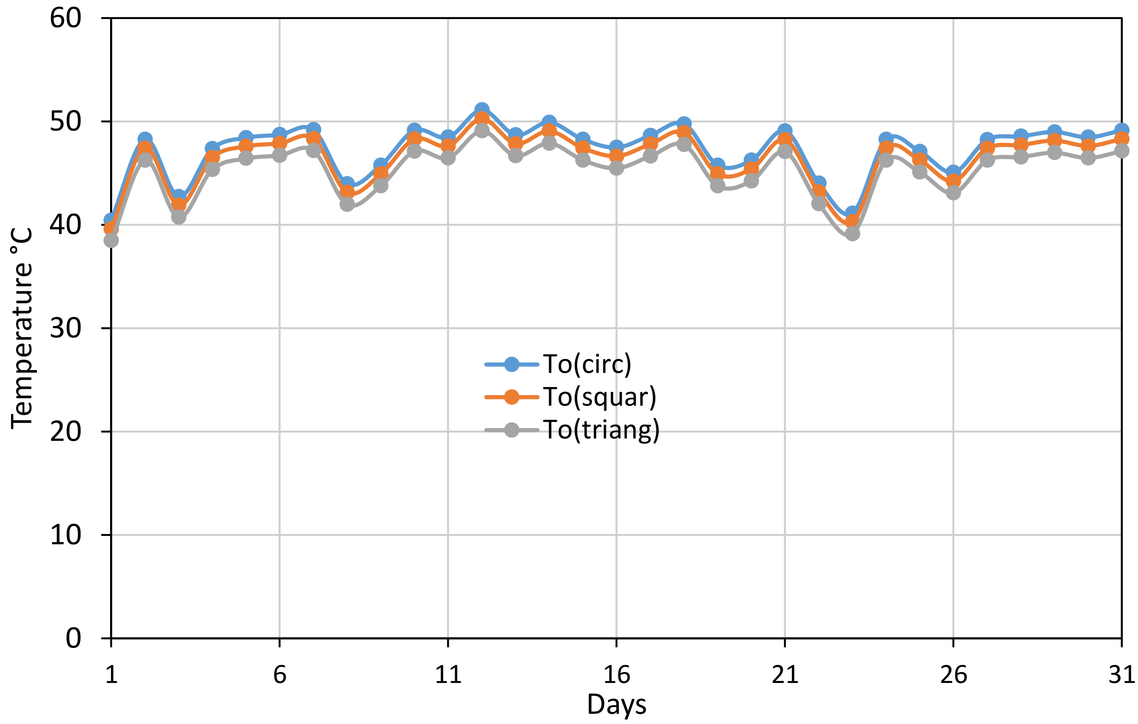

Figure 6.1 Variation of outlet temperature with time for three models of collectors for (January).

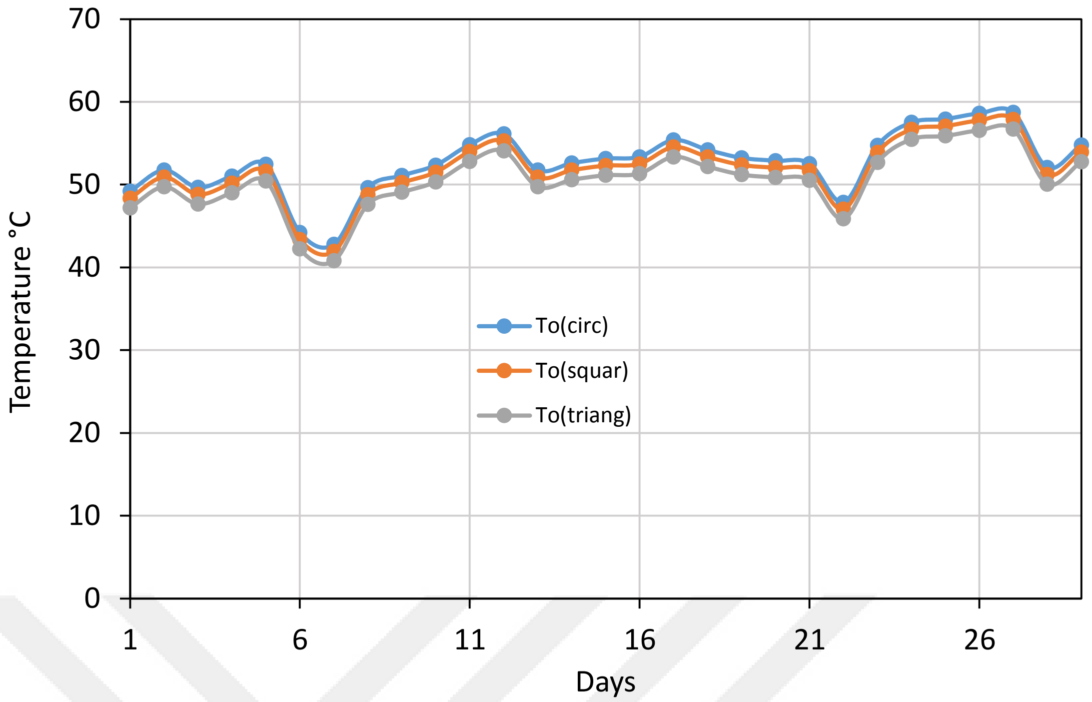

Figure 6.2 Variation of outlet temperature with time for three models of collectors for (February).

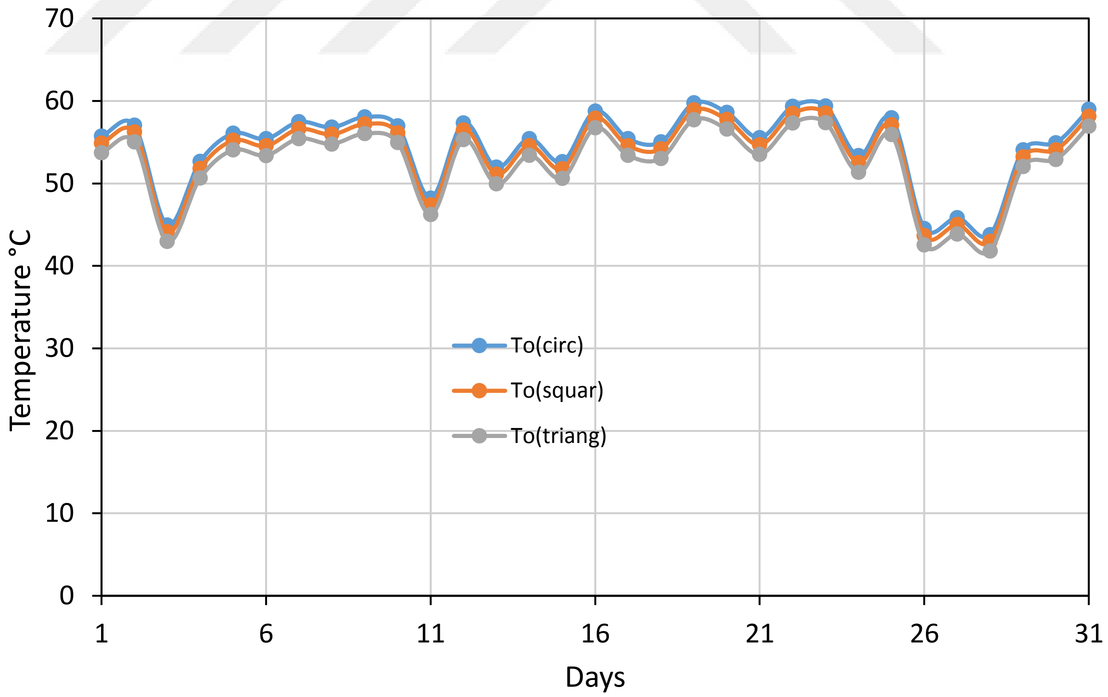

Figure 6.3 Variation of outlet temperature with time for three models of collectors for (March).

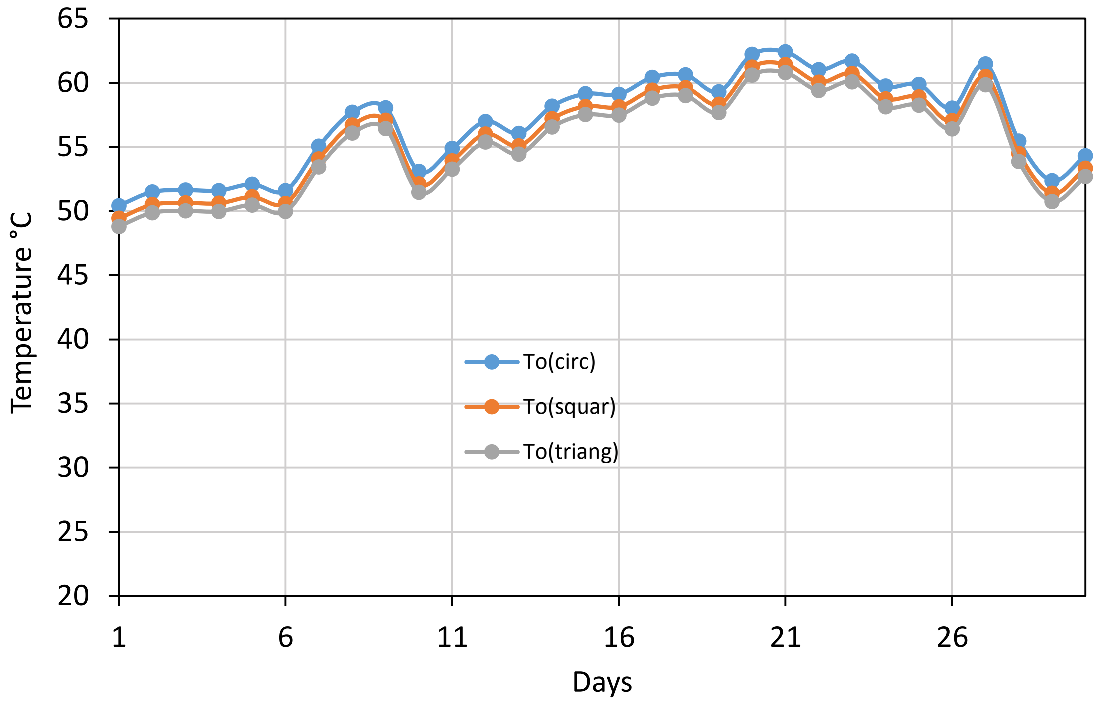

Figure 6.4 Variation of outlet temperature with time for three models of collectors for (April).

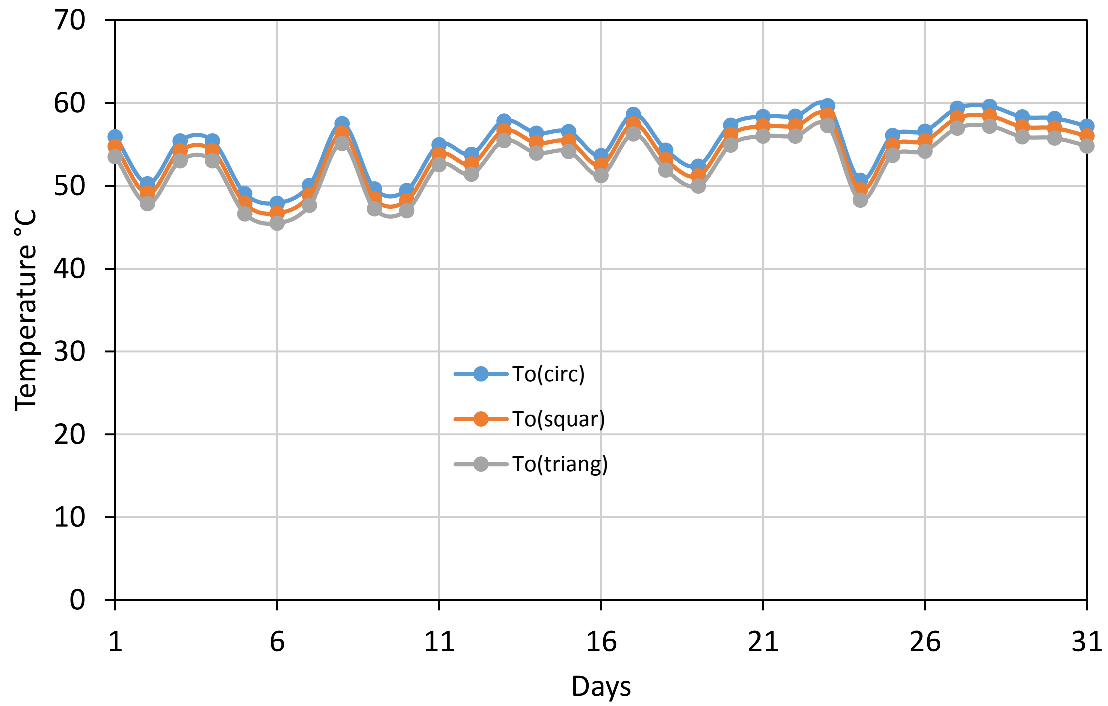

Figure 6.5 Variation of outlet temperature with time for three models of collectors for (May).

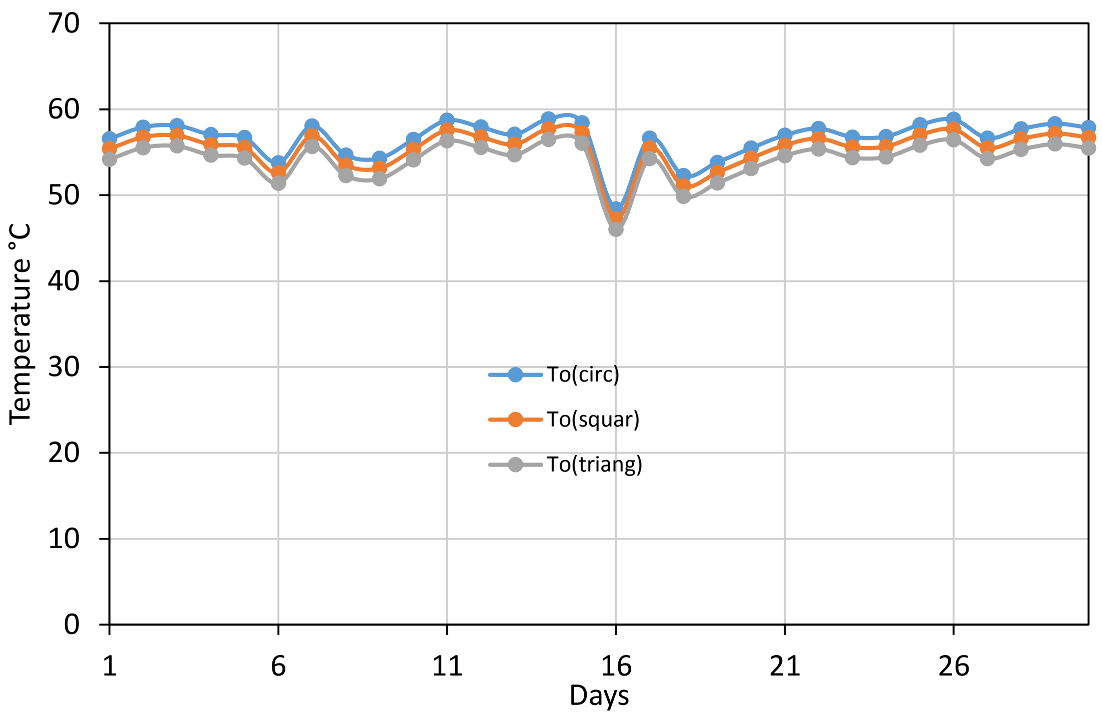

Figure 6.6 Variation of outlet temperature with time for three models of collectors for (June).

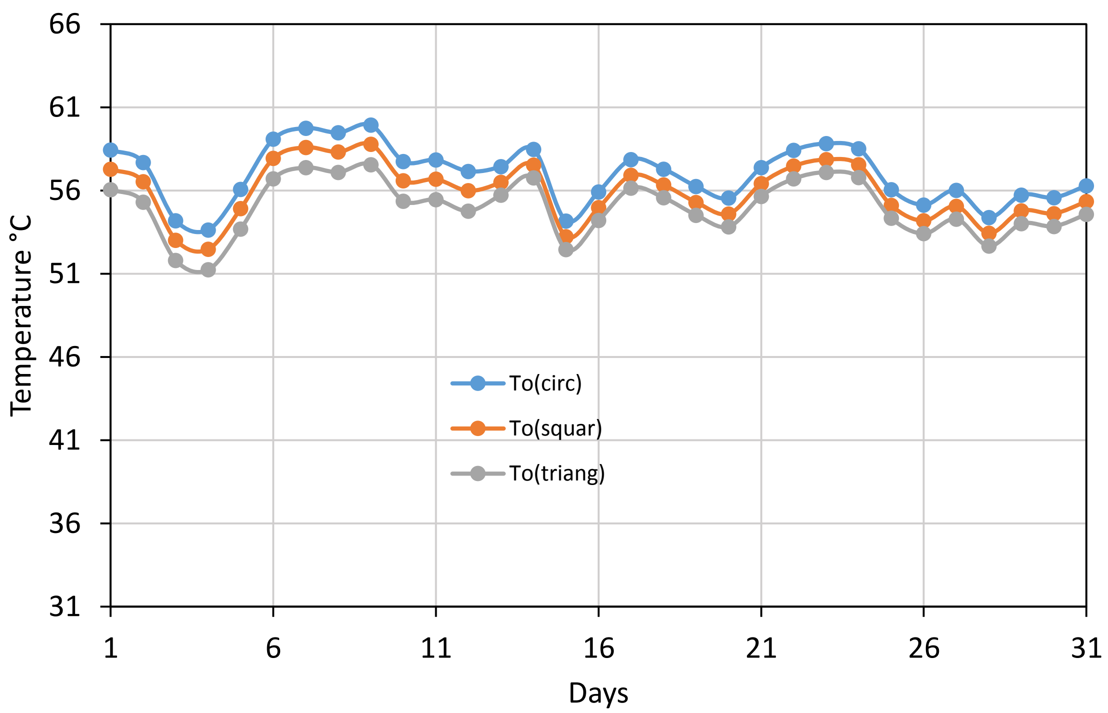

Figure 6.7 Variation of outlet temperature with time for three models of collectors for (July).

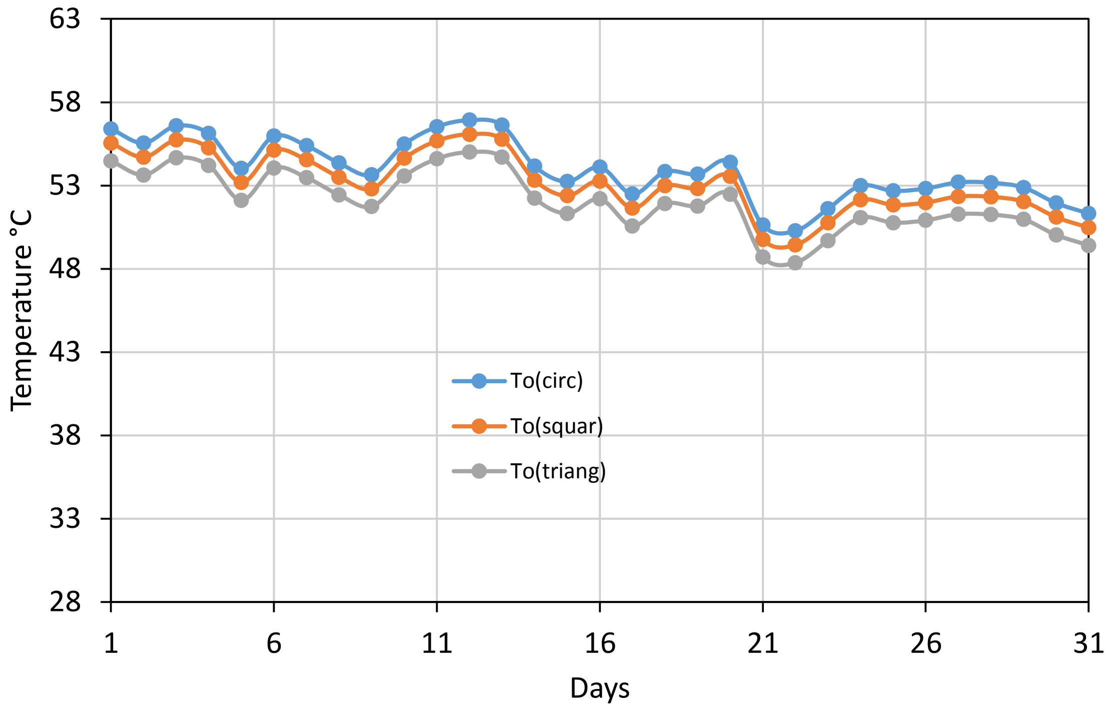

Figure 6.8 Variation of outlet temperature with time for three models of collectors for (August).

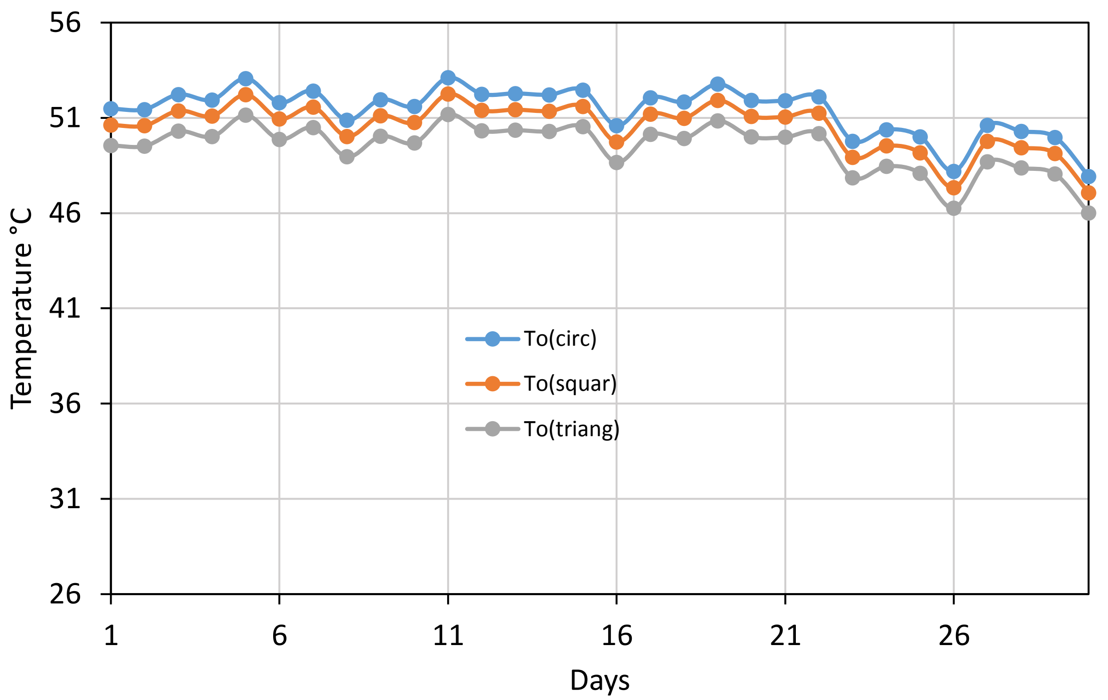

Figure 6.9 Variation of outlet temperature with time for three models of collectors for (September).

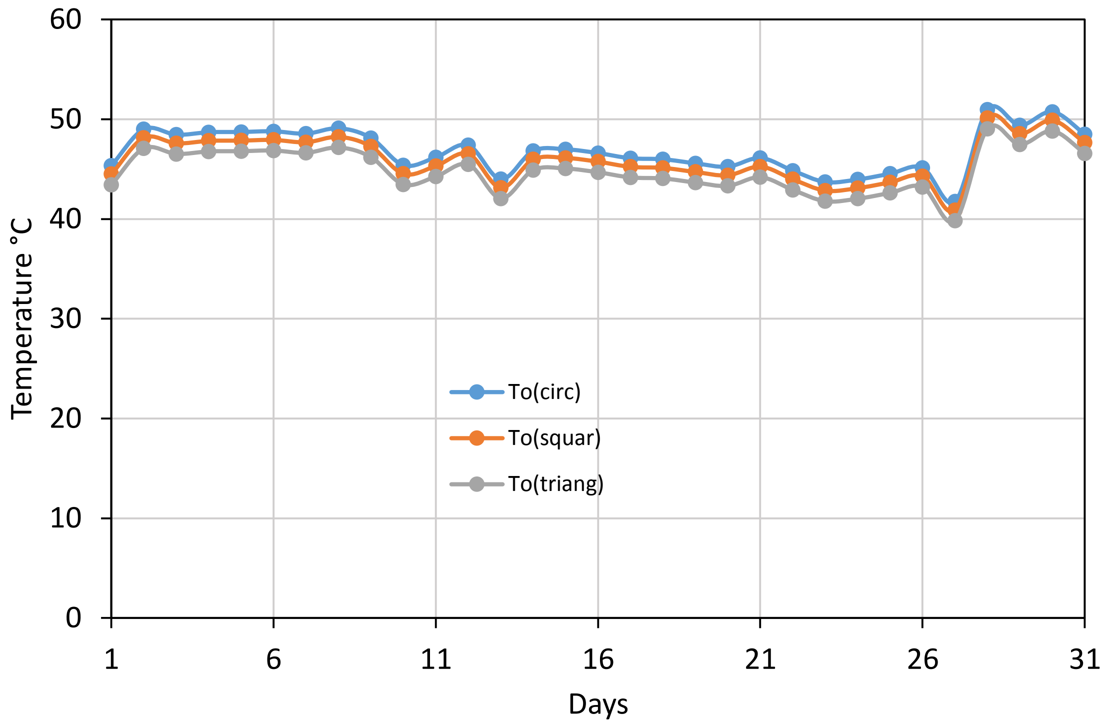

Figure 6.10 Variation of outlet temperature with time for three models of collectors for (October).

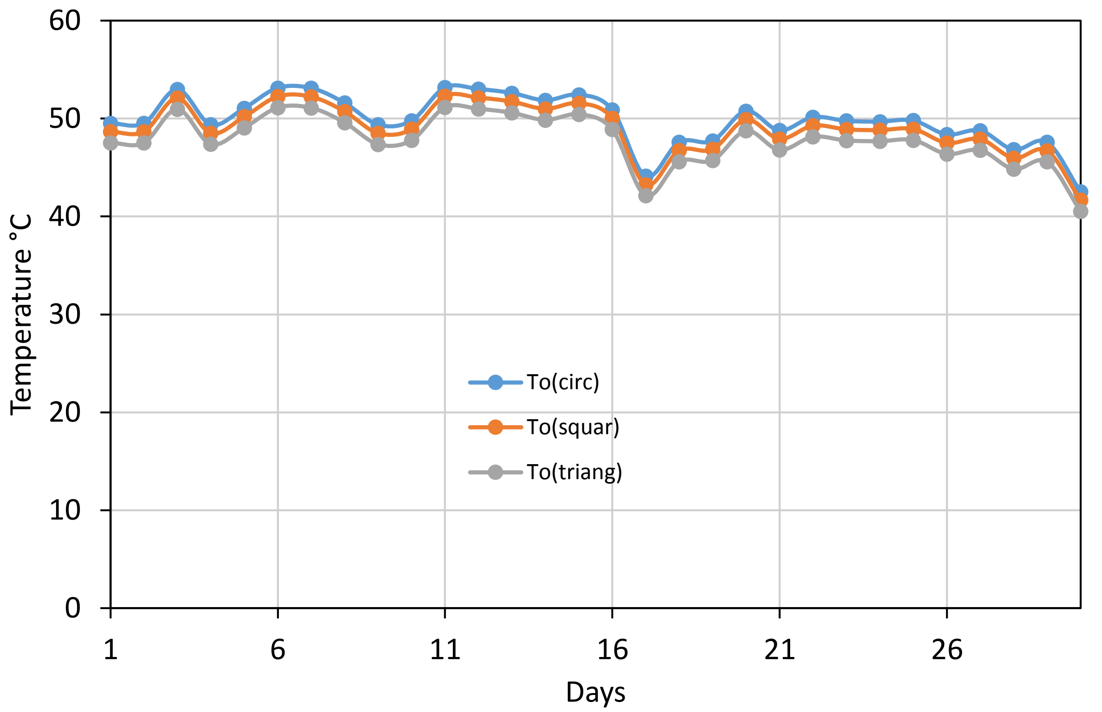

Figure 6.11 Variation of outlet temperature with time for three models of collectors for (November).

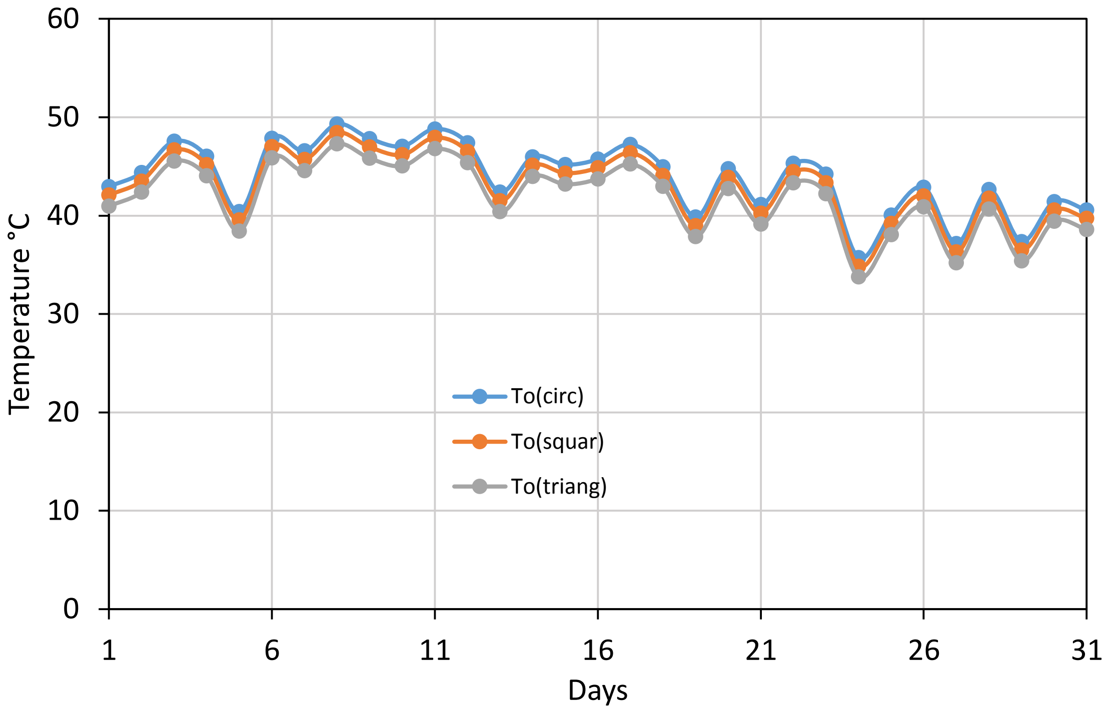

Figure 6.12 Variation of outlet temperature with time for three models of collectors for (December).

6.3.3 Collector Efficiency

The efficiency of the flat-plate solar collector (η_c) is define as the ratio of the rate of useful energy supplied by the collector (Q_u) to the rate of incident solar energy in its area. The instantaneous efficiency of the collector with time for three type of flat plate solar collectors. The instantaneous efficiency increases from the first hour at sunrise due to the increment in the incident solar radiation until it reaches its maximum value at (12:00 PM or 13:00 PM) and then start to decrease at the afternoon hours, this because of the decreasing of the incident solar radiation. The decrement of the efficiency at the afternoon hours was slowly. These Figures (6.13), (6.14), (6.15), (6.16), (6.17), (6.18), (6.19), (6.20), (6.21), (6.22), (6.23) and (6.24) show the Variation of efficiency with time for three model of collectors which were circular, square and triangle, from January to December. Then the difference between the efficiencies of the three types because the difference in the surface area which be under the solar intensity.

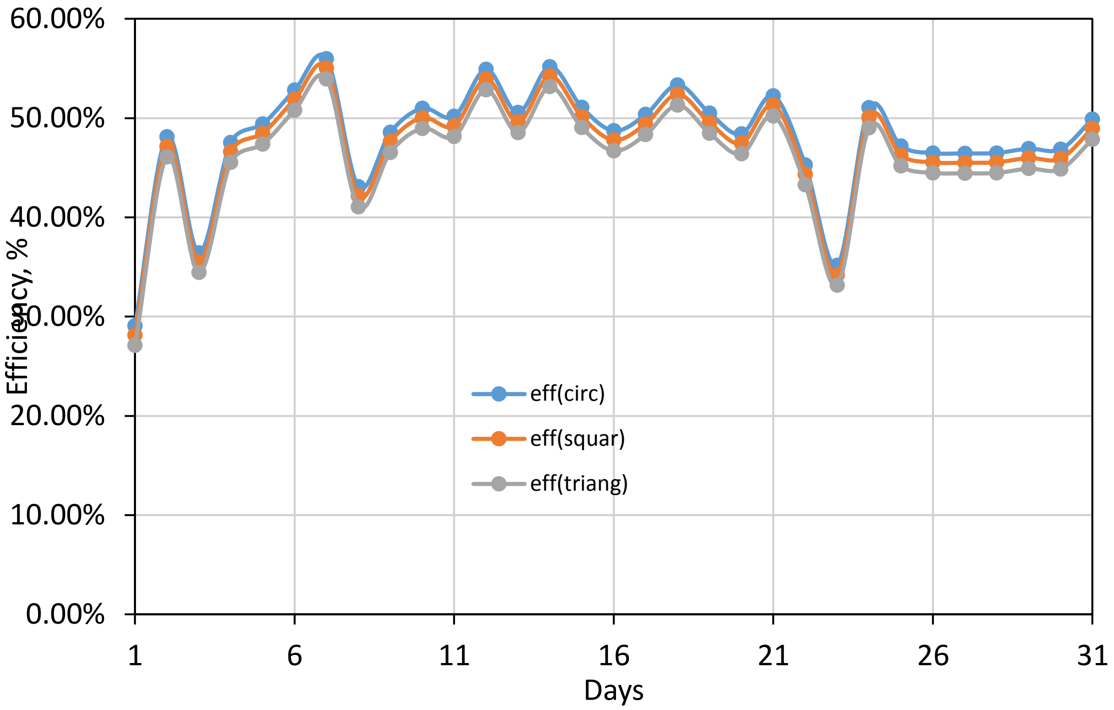

Figure 6.13 Variation of efficiency with time for three models of collectors for (January).

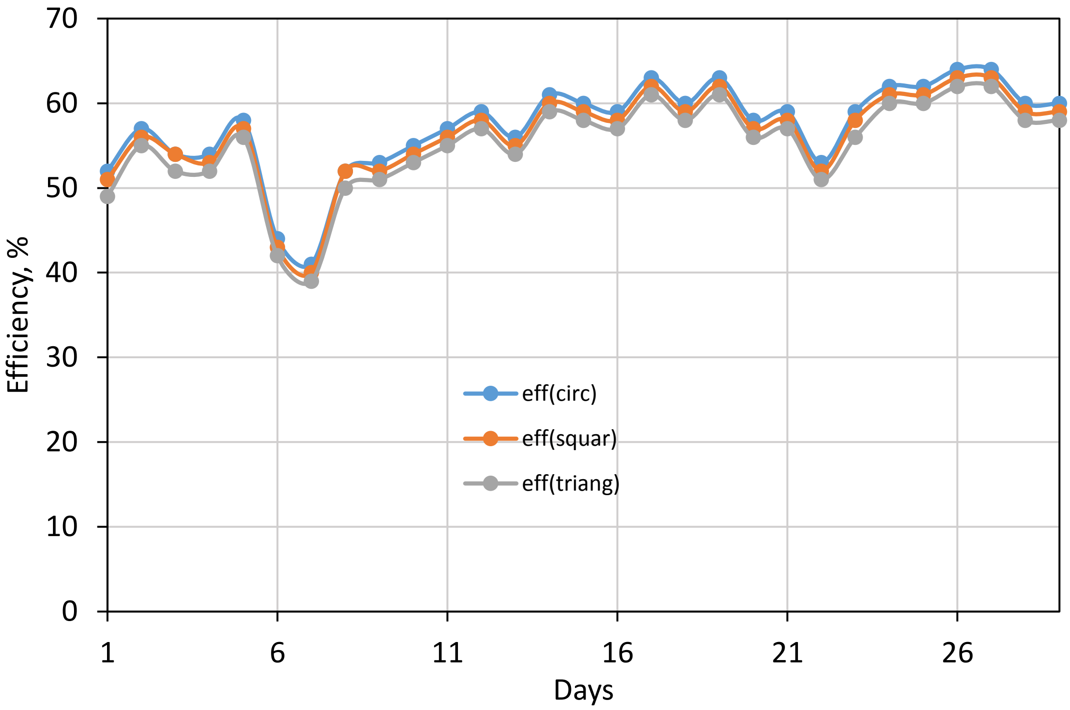

Figure 6.14 Variation of efficiency with time for three models of collectors for (February).

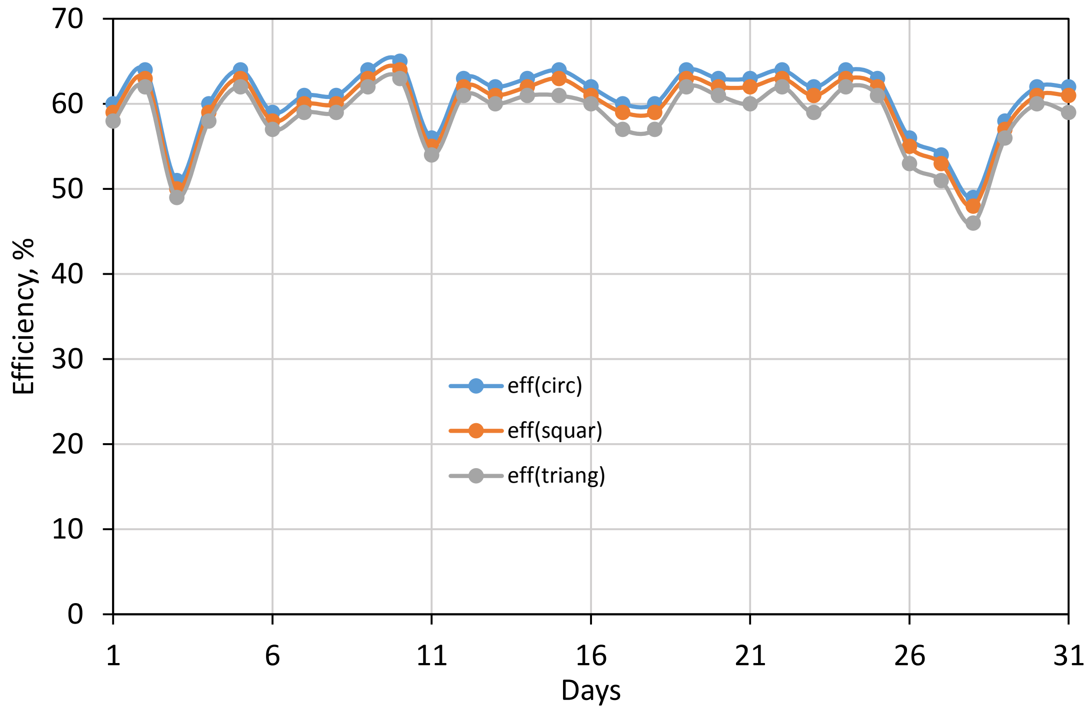

Figure 6.15 Variation of efficiency with time for three models of collectors for (March).

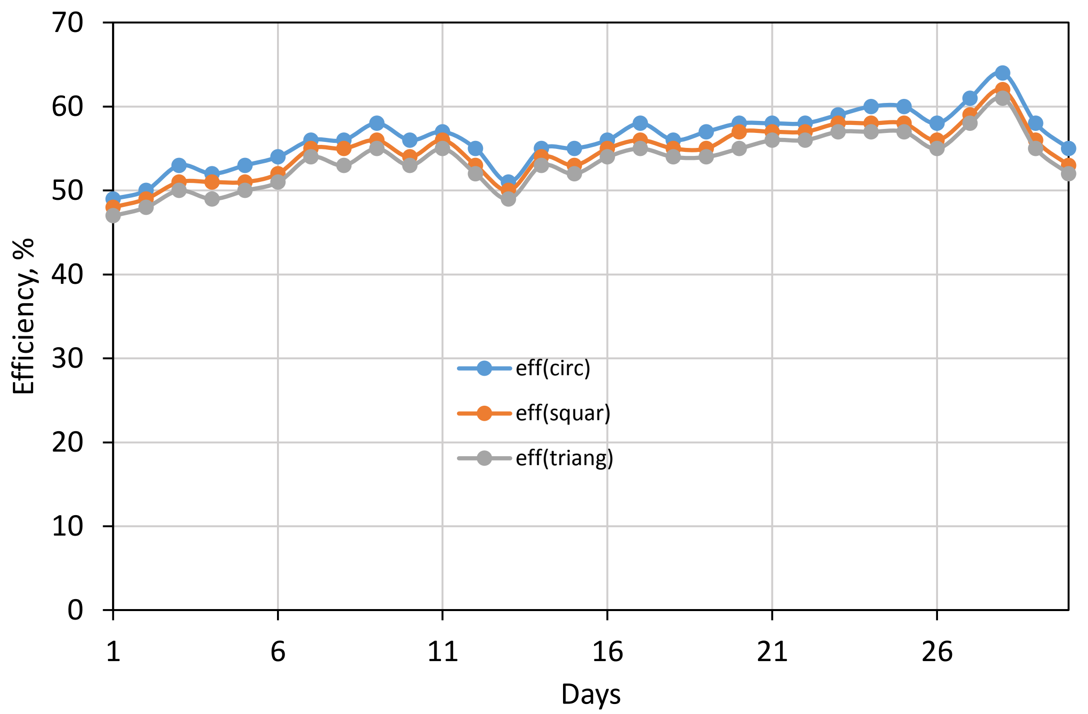

Figure 6.16 Variation of efficiency with time for three models of collectors for (April).

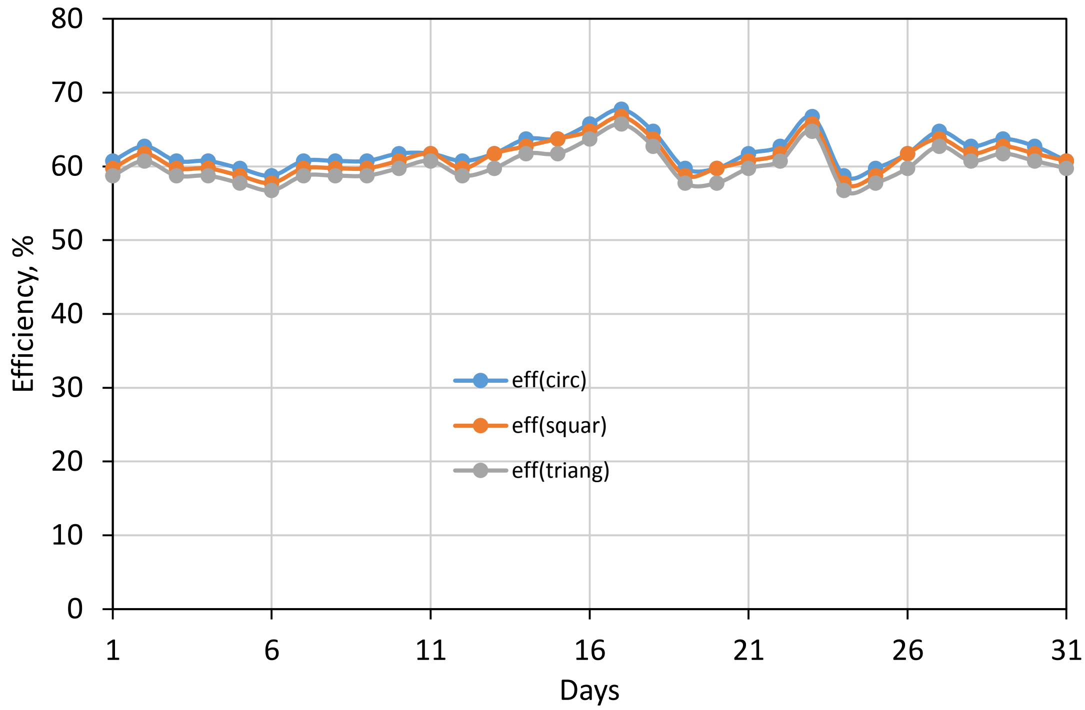

Figure 6.17 Variation of efficiency with time for three models of collectors for (May).

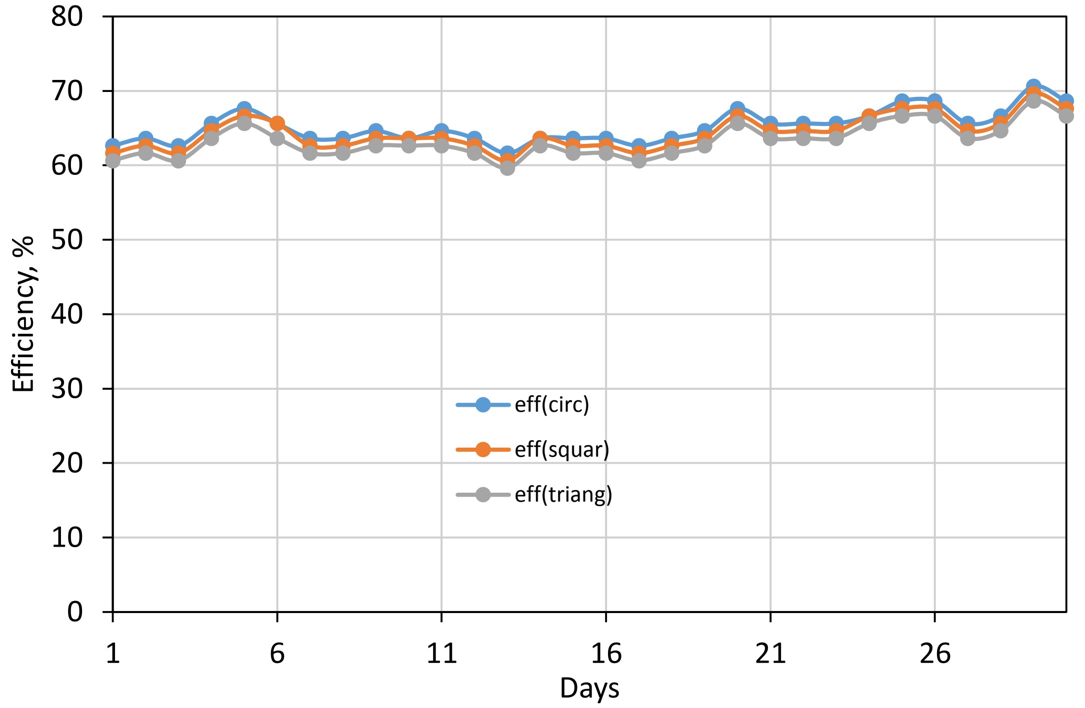

Figure 6.18 Variation of efficiency with time for three models of collectors for (June).

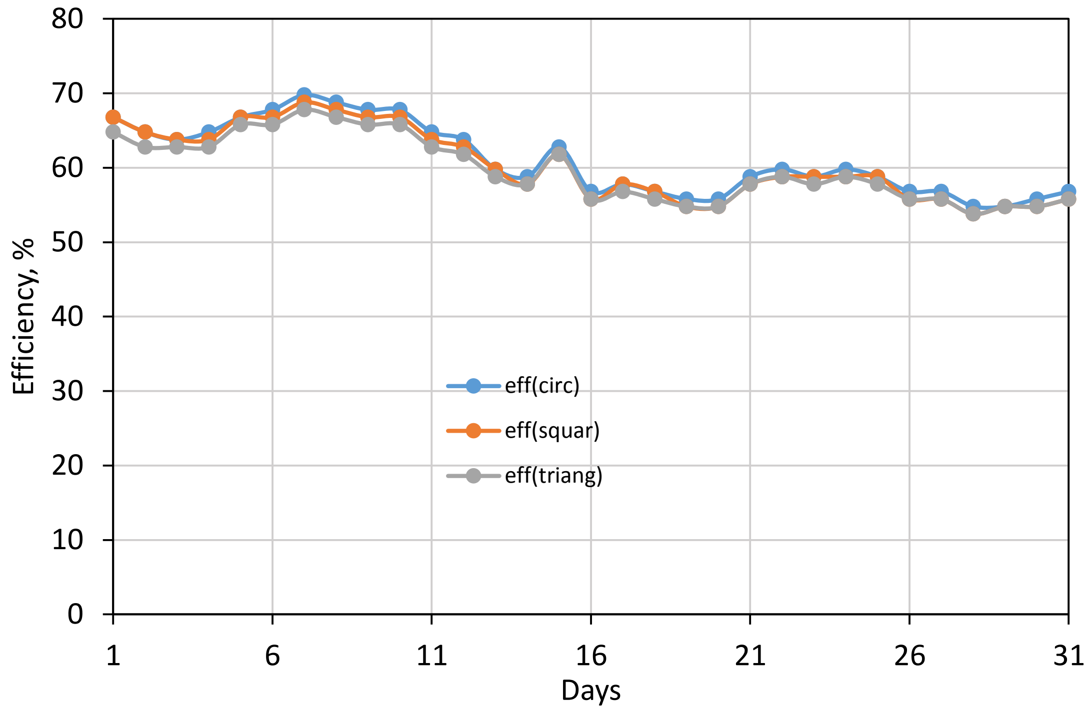

Figure 6.19 Variation of efficiency with time for three models of collectors for (July).

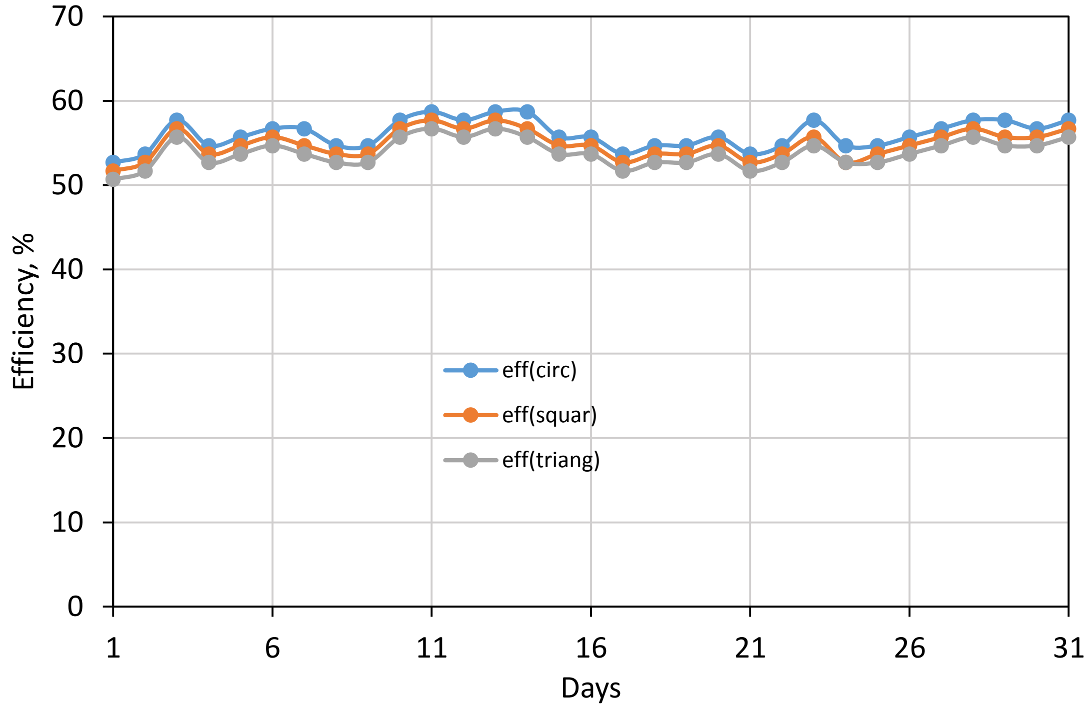

Figure 6.20 Variation of efficiency with time for three models of collectors for (August).

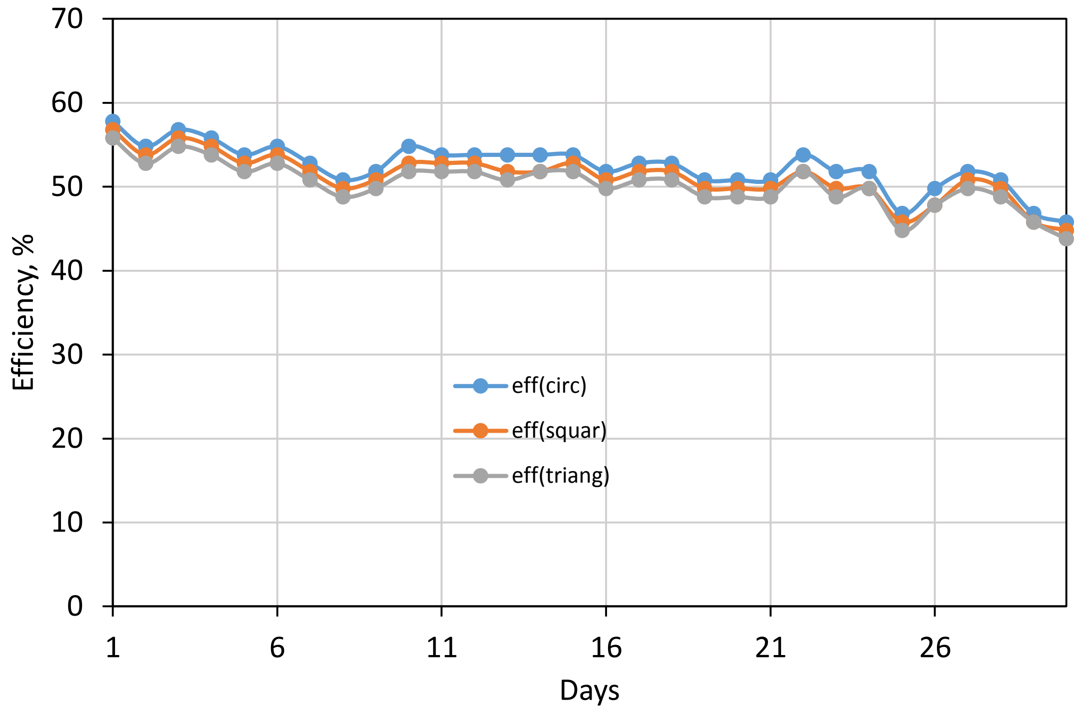

Figure 6.21 Variation of efficiency with time for three models of collectors for (September).

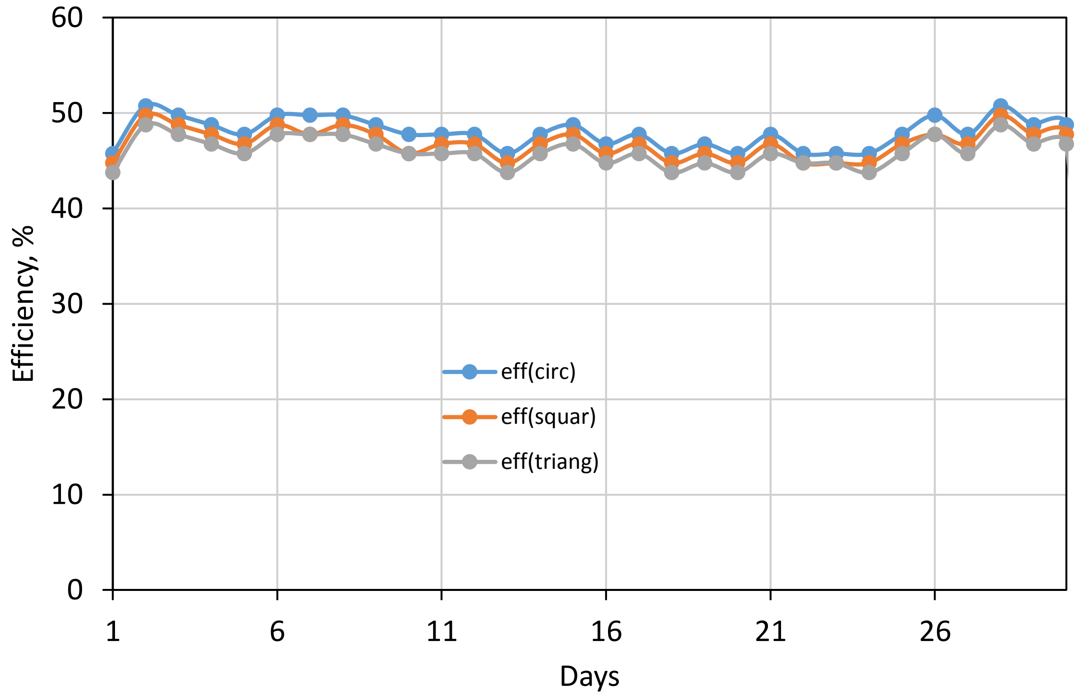

Figure 6.22 Variation of efficiency with time for three models of collectors for (October).

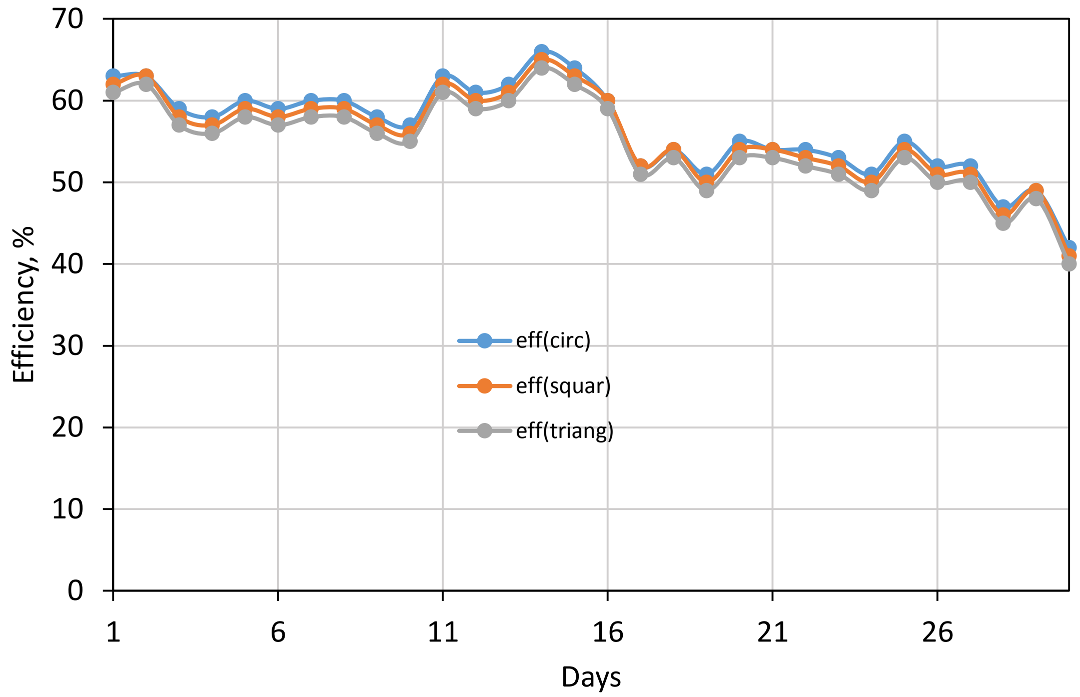

Figure 6.23 Variation of efficiency with time for three models of collectors for (November).

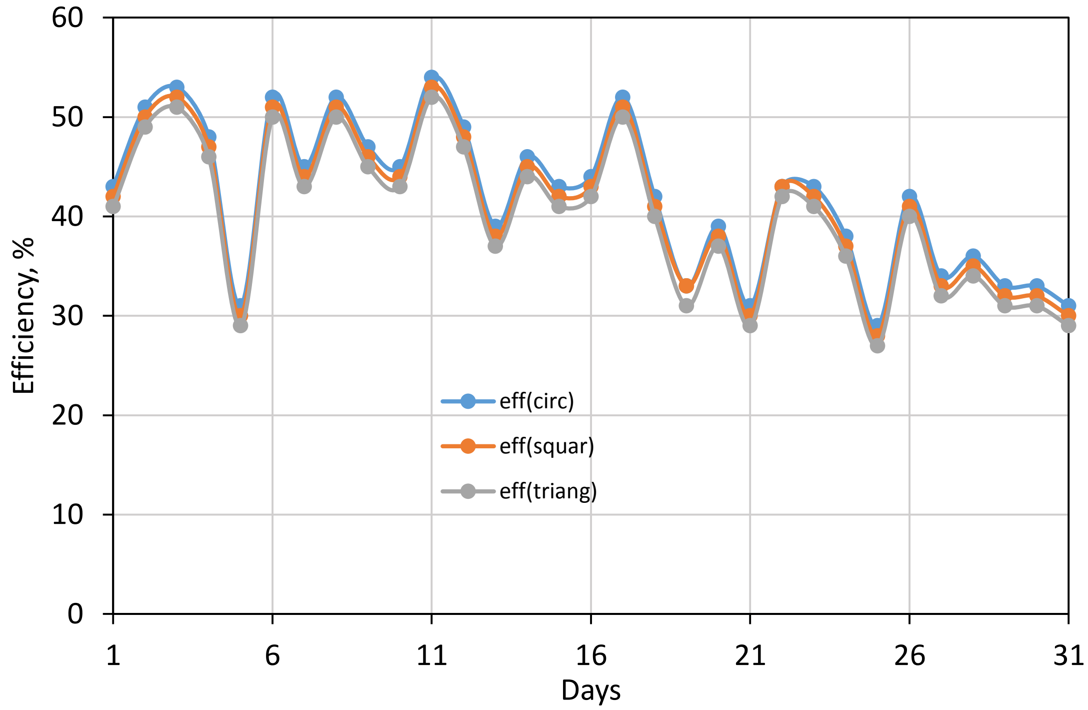

Figure 6.24 Variation of efficiency with time for three models of collectors for (December).

6.3.4 Efficiency with mass flow rate

The efficiency of the collector increase by increase the mass flow rate. The below figure represent the values of mass flow rate (kg/s) and efficiency from January to December (annually) for (circular, square, triangle) tubes. Then the increasing in the efficiency because the increase the useful gain energy which increases by increase the mass flow rate according to the useful gain energy equation in chapter 3. These Figures (6.25), (6.26), (6.27), (6.28), (6.29), (6.30), (6.31), (6.32), (6.33), (6.34), (6.35) and (6.36) show the Variation of efficiency with mass flow rate for three model of collectors which were circular , square and triangle from January to December.

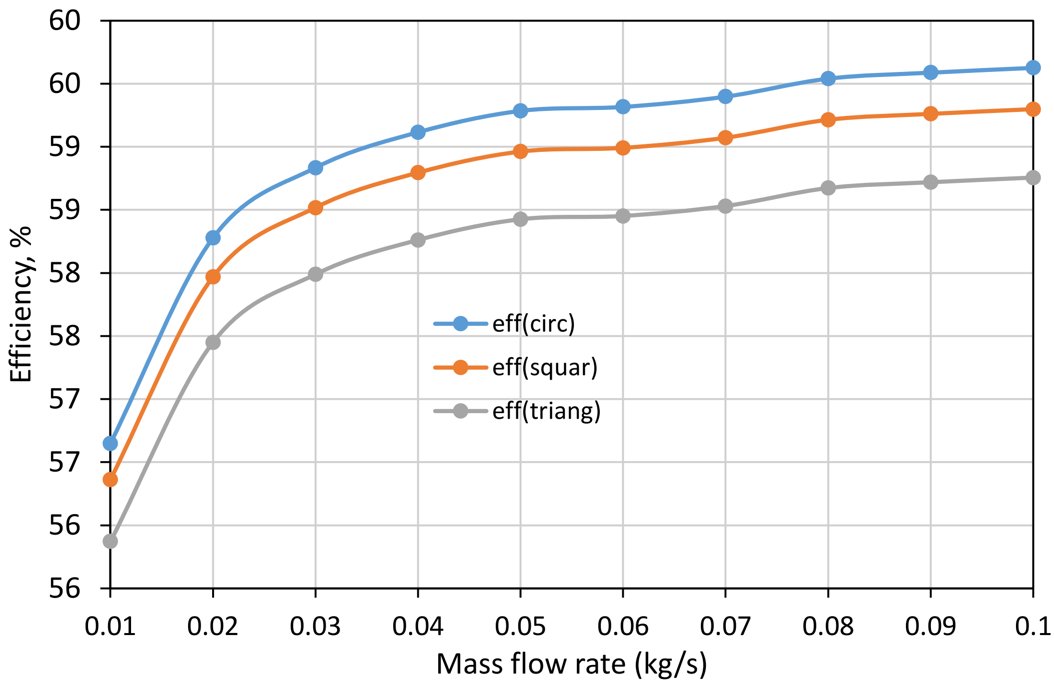

Figure 6.25 Variation of mass flow rate (kg/s) and efficiency (January).

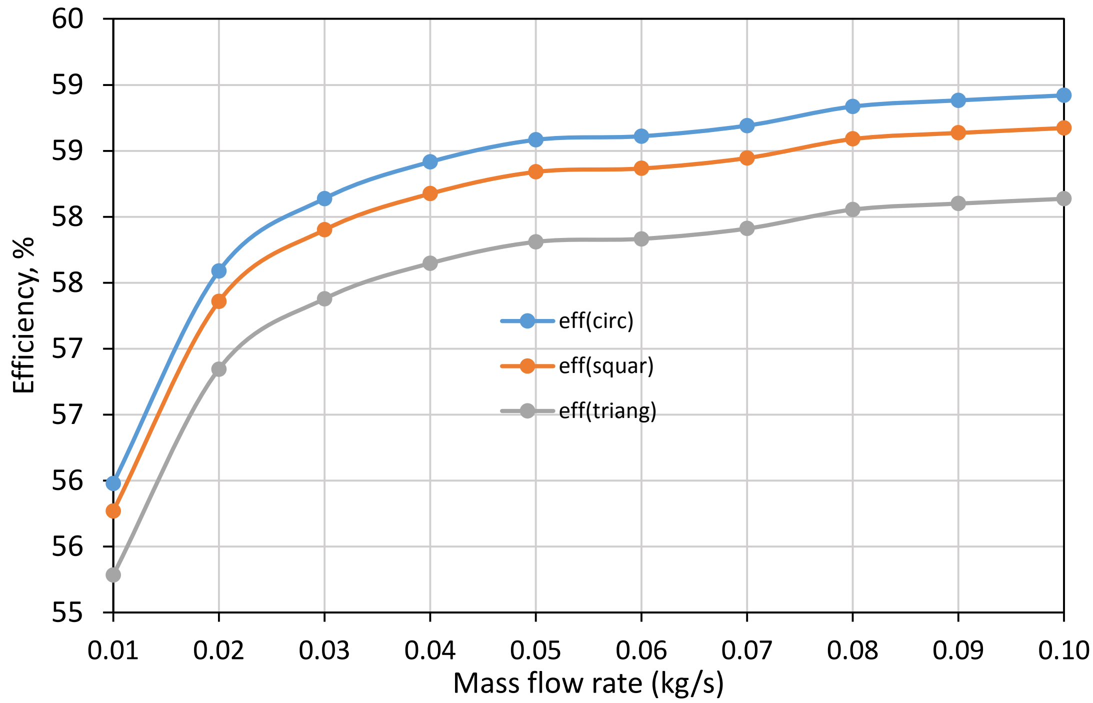

Figure 6.26 Variation of mass flow rate (kg/s) and efficiency (February).

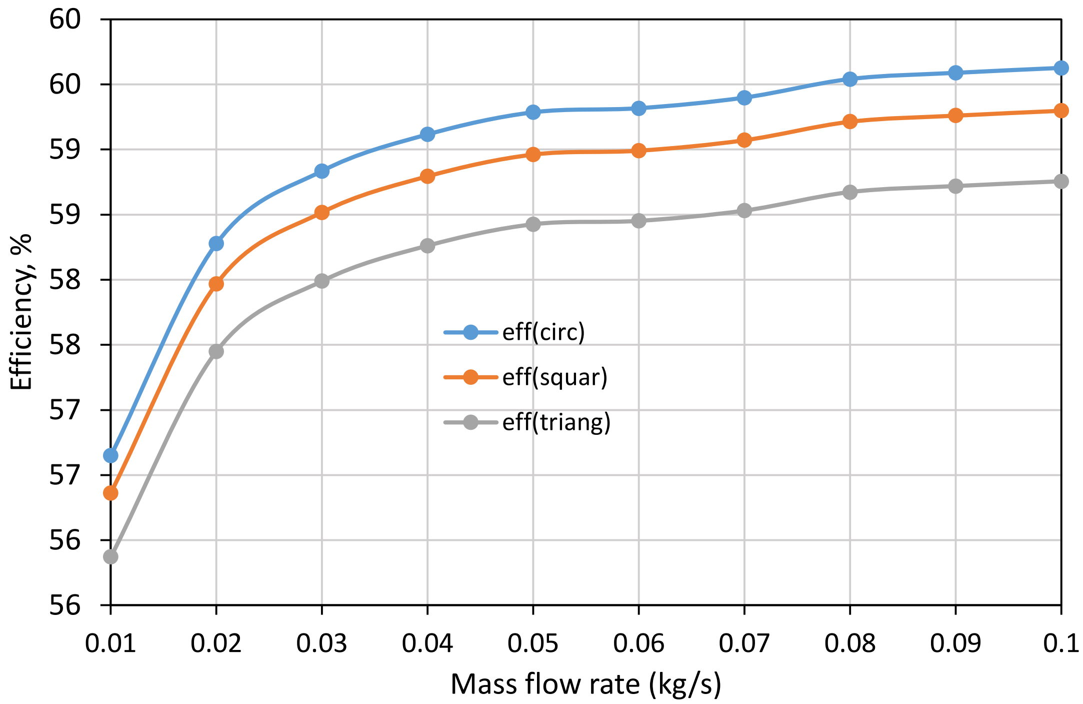

Figure 6.27 Variation of mass flow rate (kg/s) and efficiency (March).

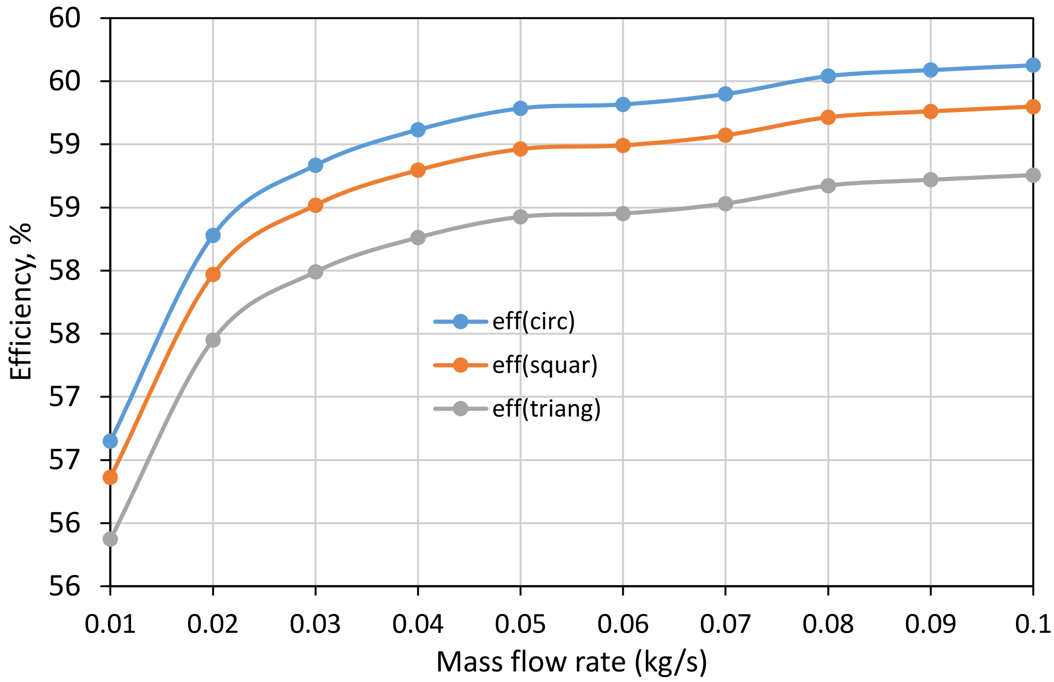

Figure 6.28 Variation of mass flow rate (kg/s) and efficiency (April).

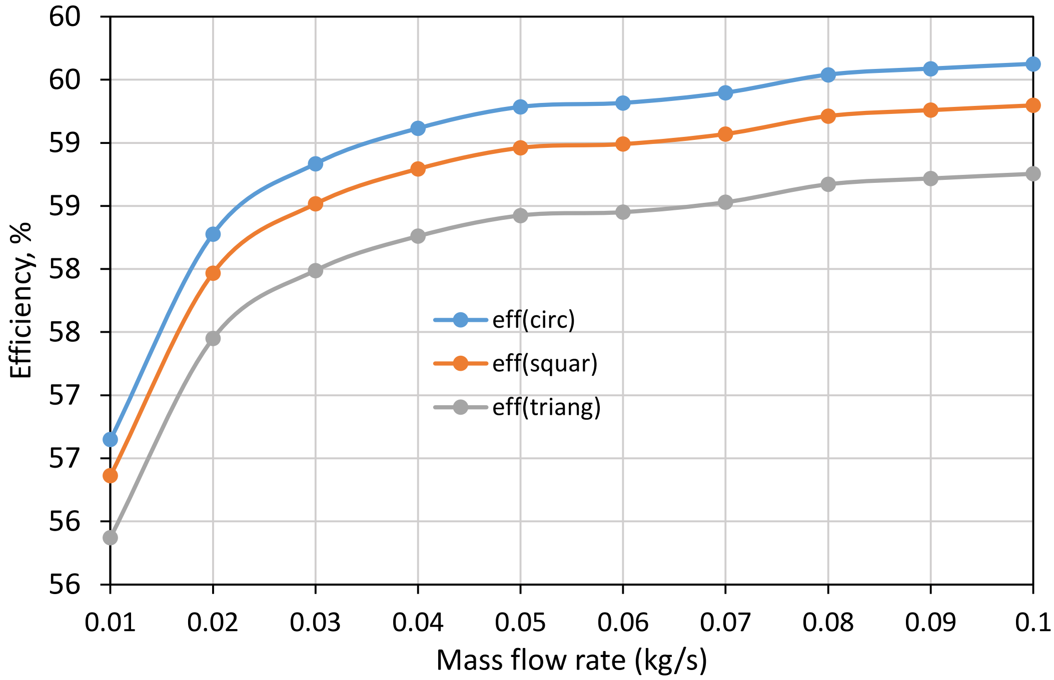

Figure 6.29 Variation of mass flow rate (kg/s) and efficiency (May).

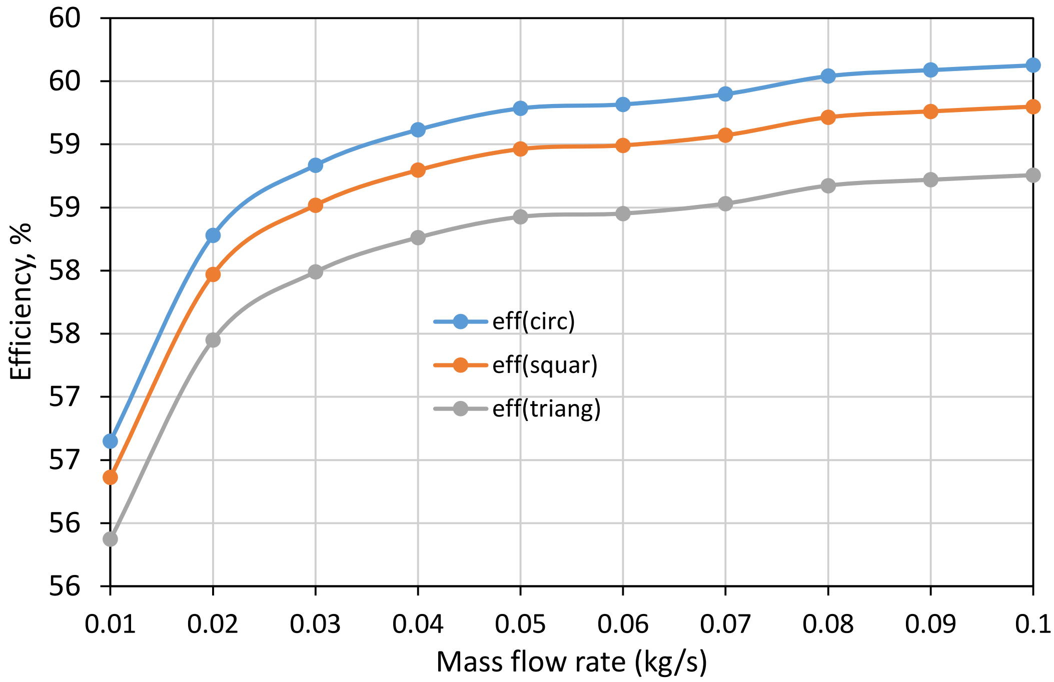

Figure 6.30 Variation of mass flow rate (kg/s) and efficiency (June).

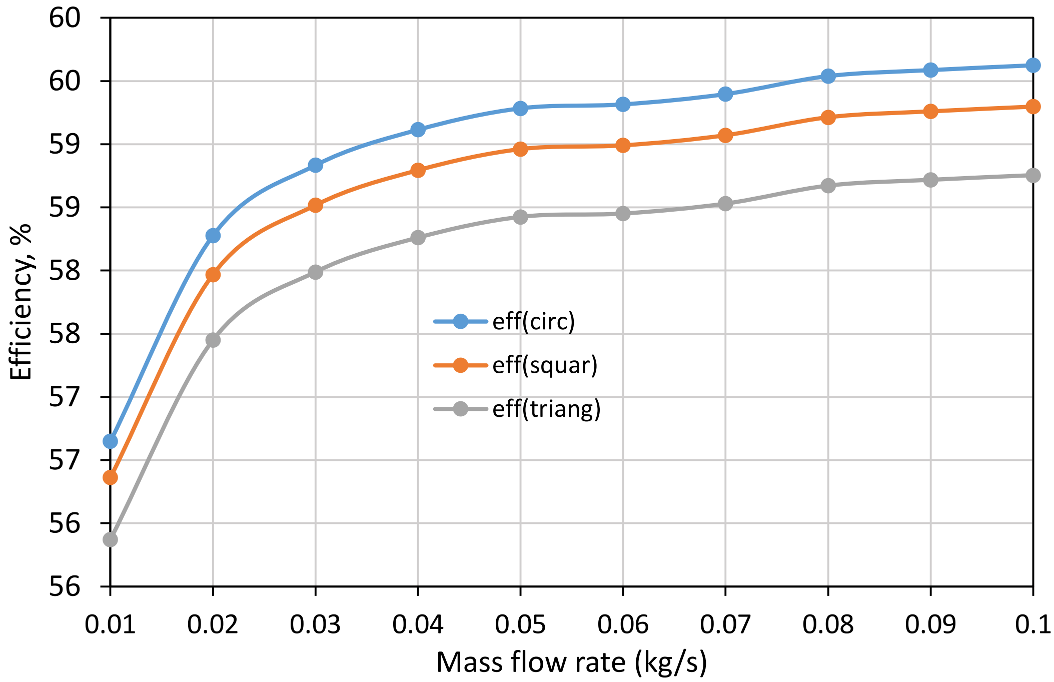

Figure 6.31 Variation of mass flow rate (kg/s) and efficiency (July).

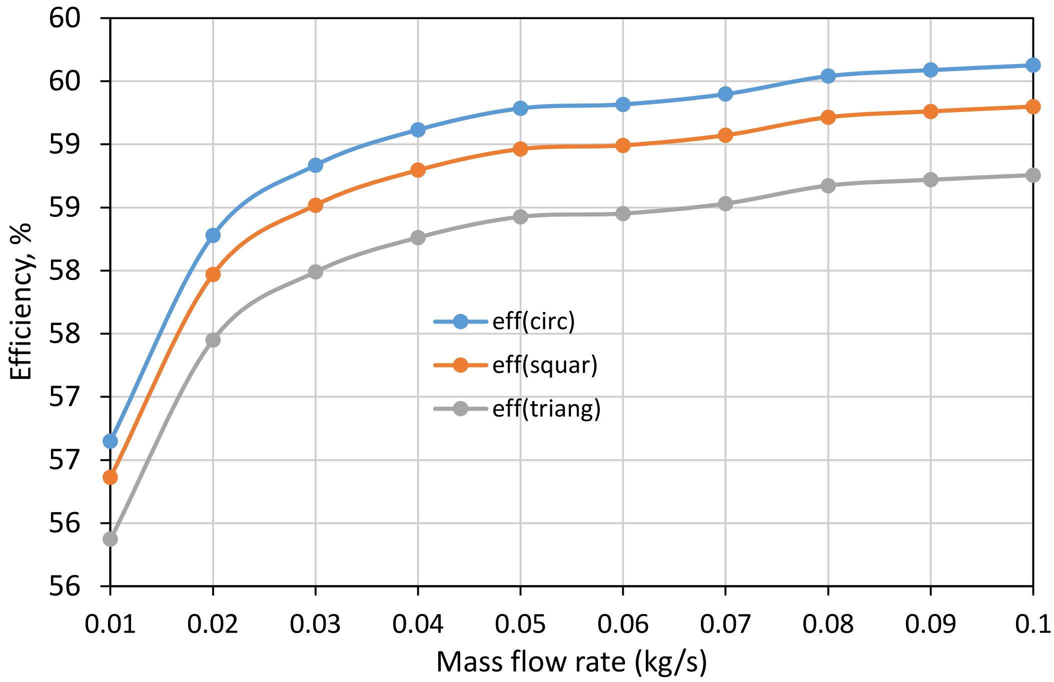

Figure 6.32 Variation of mass flow rate (kg/s) and efficiency (August).

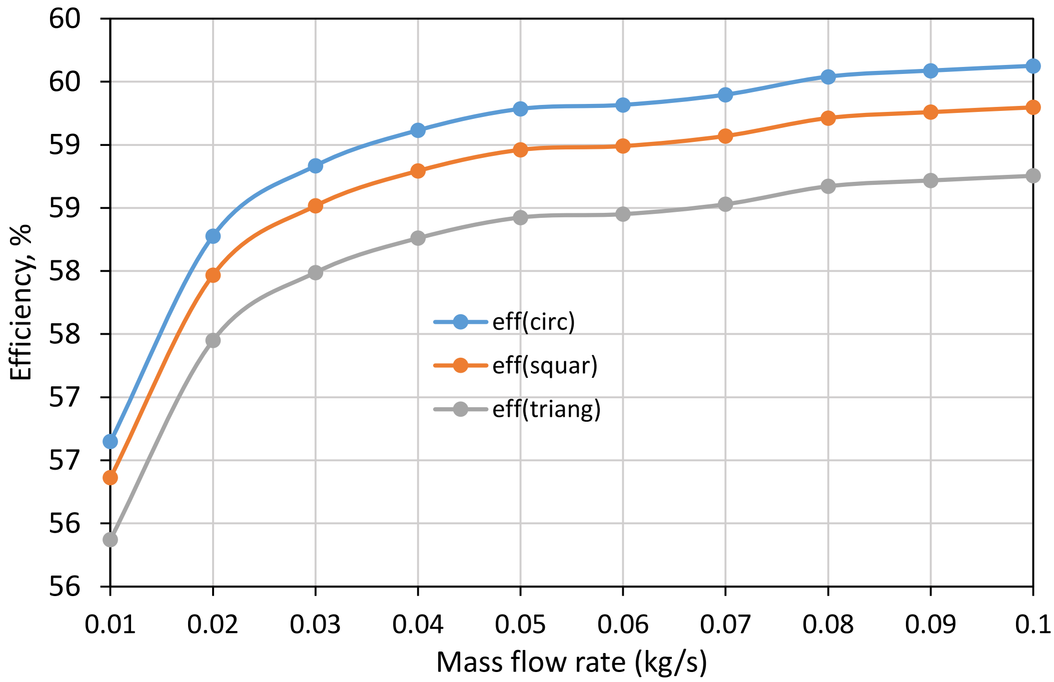

Figure 6.33 Variation of mass flow rate (kg/s) and efficiency (September).

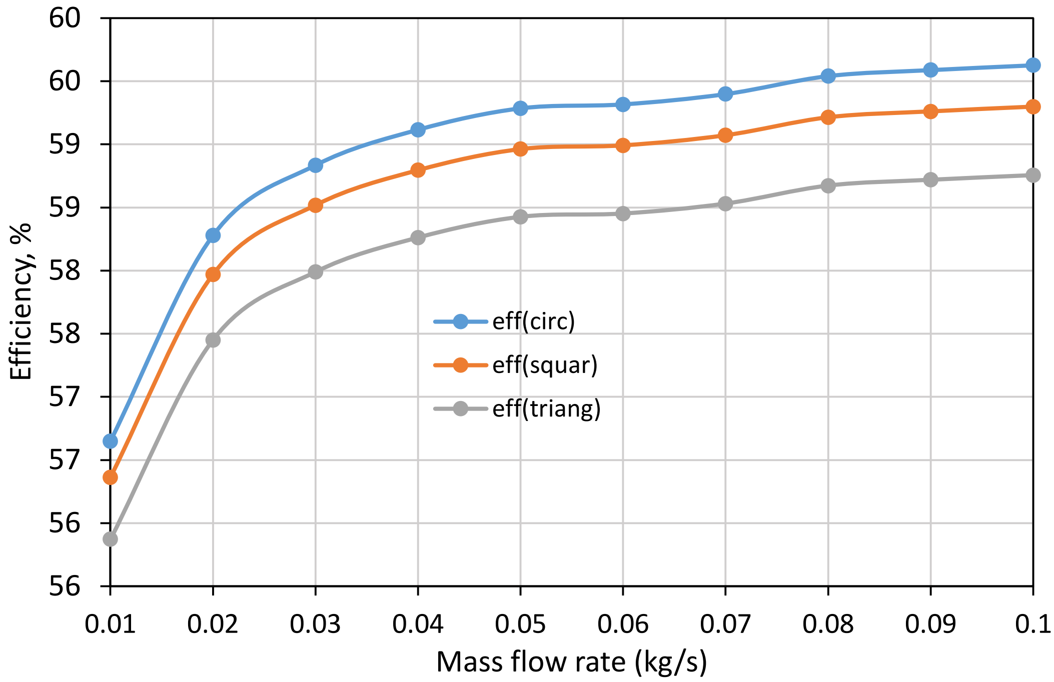

Figure 6.34 Variation of mass flow rate (kg/s) and efficiency (October).

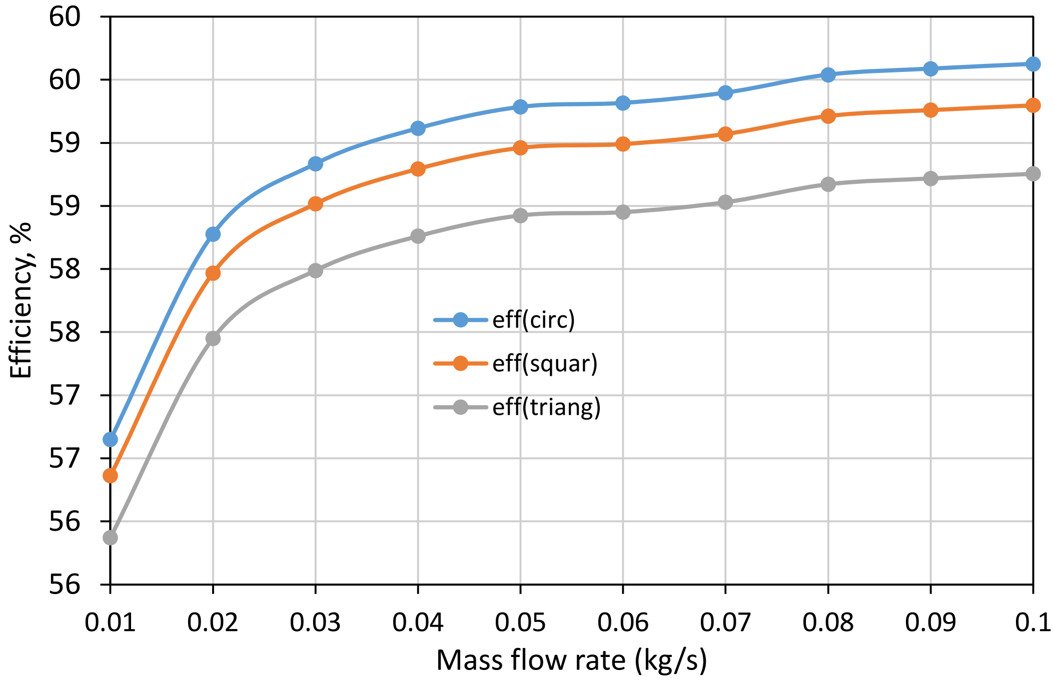

Figure 6.35 Variation of mass flow rate (kg/s) and efficiency (November).

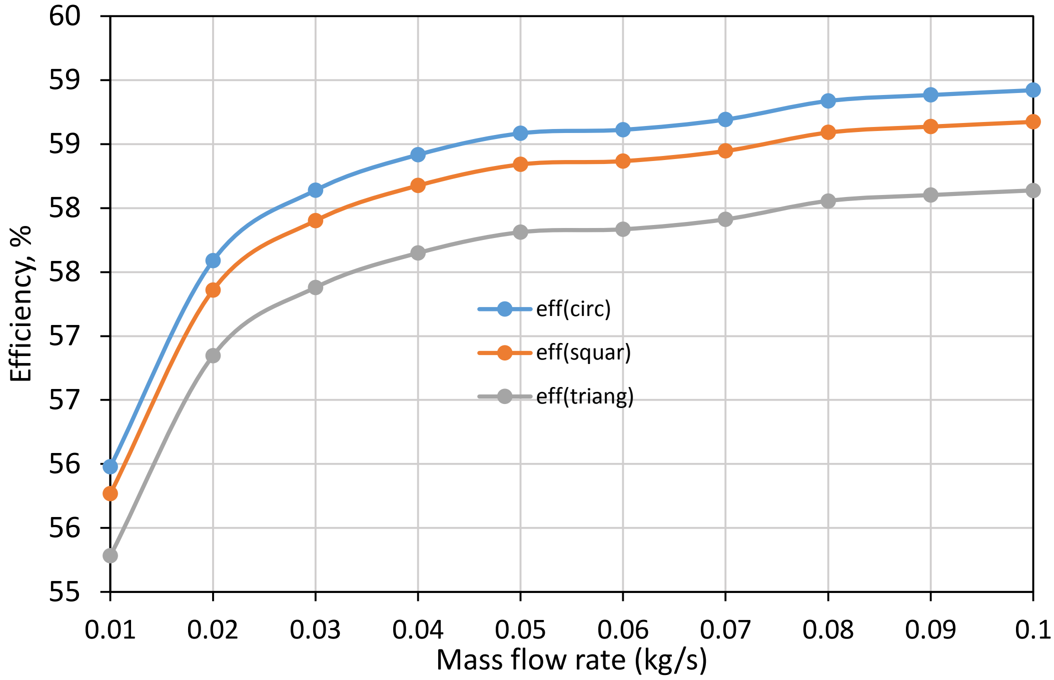

Figure 6.36 Variation of mass flow rate (kg/s) and efficiency (December).

6.4 Results for fraction load by solar energy

the annual and monthly load for flat plate solar collector that use for service water heating system after that we can select the optimum design based on the annual fraction thermal performance. During this study we calculated the fraction load for the optimum type of flat plate solar collector. The flat plate solar collector type circular was optimum then after selected the optimum type then must select the optimum design for the flat plate solar collector based on the relation between the fraction load and collector area the relationship of the optimum area to the annual thermal performance will be calculated then the optimum area occurs where the slope of the curve is $P2\ C_A/P1\ C_{F1}\ L$.

6.4.1 Annually Fraction load for different collector areas

By calculating the fraction load by solar energy for whole year with a several collector area that give us hence which design of collector optimum. The select the optimum design will be based on the fraction thermal performance calculation for several collector areas. A computer program was prepared in Matlab in order to carry out all the numerical calculations which are the calculations of the fraction load and the monthly load the calculation repeated for each hour from sunrise to the sunset for whole year. The collector area used as input data for different values. The relationship of the optimum area to the annual thermal performance was calculated then the optimum area occurred at the slope of the curve is $P2\ C_A/P1\ C_{F1}\ L$. Figure 6.37 shows the variation annually fraction load by solar energy with collector area obtained in the present study for annual fraction load. The figure shows that the annual fraction load values for different collector areas which increase with increase the collector area this first reason shows the validity of the solution method presented in this study. The second reason the value was calculated in $P2\ C_A/P1\ C_{F1}\ L$ equation the same value was calculated from the slope equation then that indicates the validity of the solution in this study where the value was calculated from $P2\ C_A/P1\ C_{F1}\ L$ was 0.0279 and the value obtained from the slope equation 0.0281 where the collector area Ac is about 4 m^2. As a results, it is observed that this figure indicates validity of the present solution in this study for fraction load analysis. Then the other calculations for all areas represent and obtained in the same procedure as a tables in appendix B

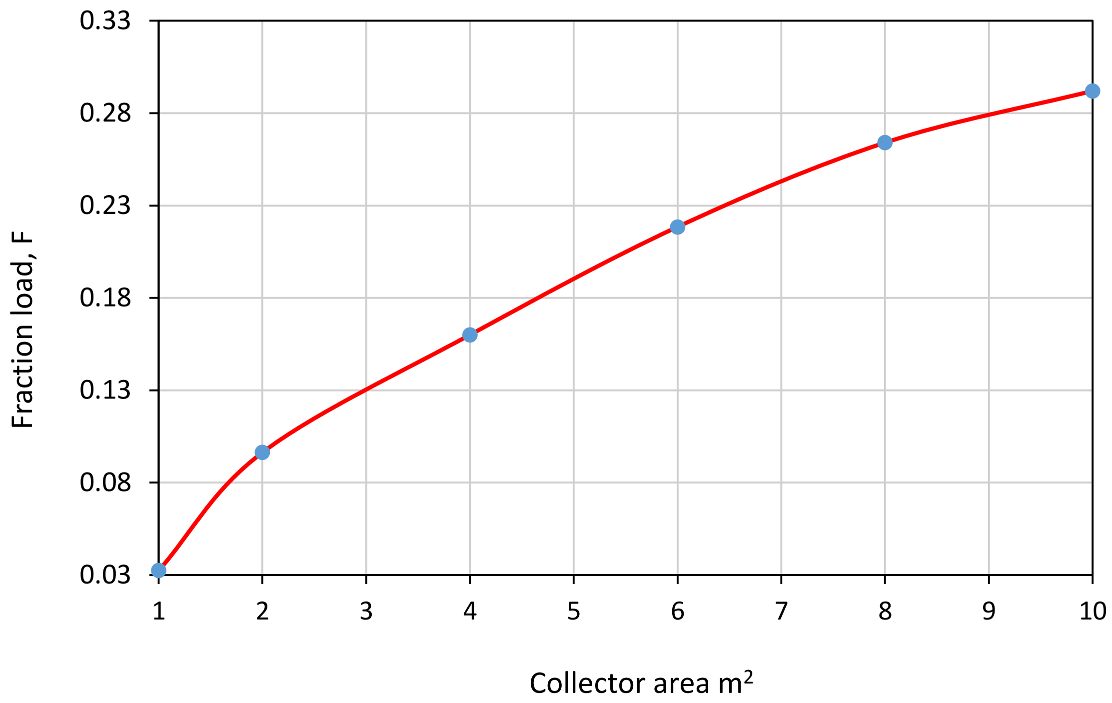

Figure 6.37 Variation annually fraction load by solar energy with collector area

6.4.2 f-chart method and f-calculation

The f-chart calculation for the circular flat plate solar collector for whole year from January to December. The outline the f-chart method for estimating the annual thermal performance of active heating systems for the building that using the liquid as a working fluid the f-chart method provides a means for estimating the fraction of annual heating load that will be supplied by the solar energy for heating system then the primary design variable is a collector area the secondary variable is a collector type, storage capacity, fluid flow and the load. The values of the f-chart and the values of the f-calculation obtained in this study of the f-chart analysis. Figure 6.38 shows variation of f-chart values and the obtained in the present study for the f-calculation. The figure shows that the f-chart values taken from f-chart method and calculated f-method for the circular flat plate solar collector are closer to each other. Match of the figure shows validity of the solution method in this study and analysis. As a results, it is observed that this figure indicates validity of the present solution in this study for f-chart and f-calculation analysis. The figure below represent the relation and the difference between the f-char$_t$ and the f-calculation and the error percentage. The table 6.1 shows calculate annually fraction load by solar energy for collector area 1 m^2 and the comparing between f-calculation and f-chart calculation then this comparing represent the validation of the study.

Table 6.1 shows calculate annually fraction load by solar energy for collector area.

Month	L	f*L	X	Y	f-chart	fss
Jan	2.922525	0.035964	0.181086	0.023471	0.01230573	0.0114
Feb	2.733975	0.059714	0.16445	0.031807	0.02184163	0.0189
March	2.922525	0.08889	0.148486	0.039265	0.03041549	0.0272
Apr	2.82825	0.100698	0.119525	0.042556	0.0356042	0.0327
May	2.922525	0.13254	0.101891	0.05111	0.04535134	0.0421
Jun	2.82825	0.156776	0.078572	0.059665	0.05543204	0.0519
Jul	2.922525	0.151145	0.068115	0.055278	0.05171725	0.0469
Aug	2.922525	0.14377	0.073118	0.053085	0.0491939	0.0472
Sep	2.82825	0.110194	0.088094	0.043872	0.03896204	0.0363
Oct	2.922525	0.072003	0.11421	0.031368	0.0246373	0.0224
Nov	2.82825	0.041289	0.145484	0.023471	0.01459896	0.0123
Dec	2.922525	0.031232	0.161134	0.02062	0.01068667	0.0099
	ΣLi=34.5	Σf*Li=1.124				
	F=Σf*Li/ΣLi	**F=0.032**				

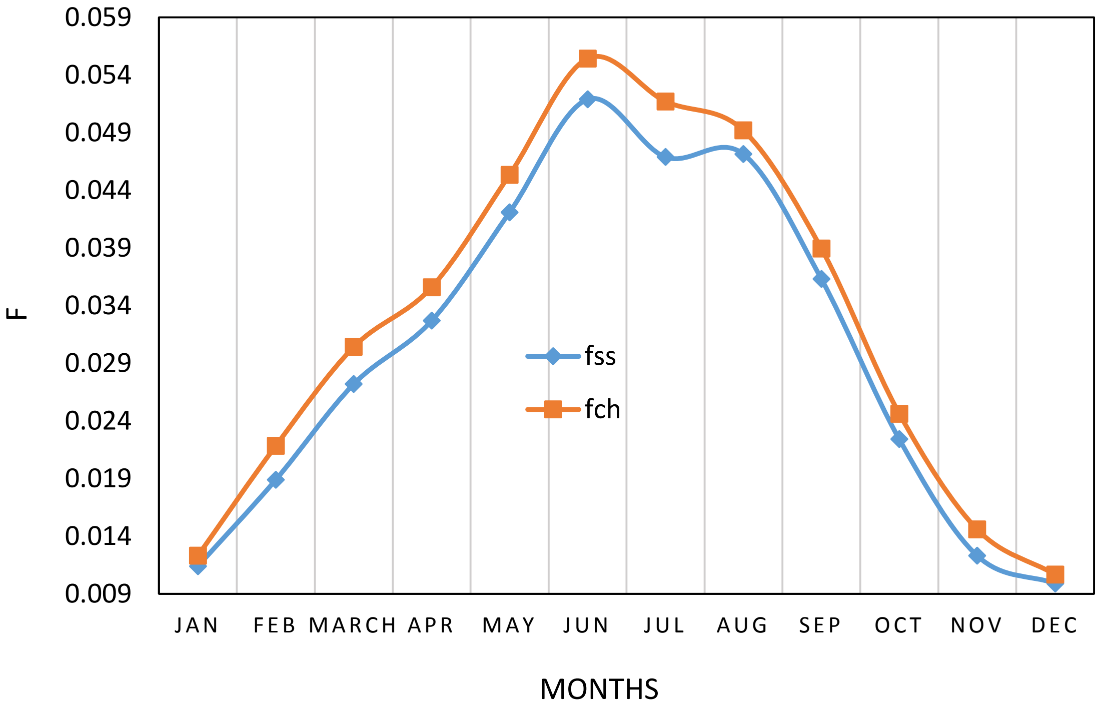

Figure 6.38 Variation between the f-chart values and f –calculation values.

6.4.3 Fraction load by solar energy with mass flow rate

In this section, the calculation of the fraction load by the solar energy for the circular, square and triangle models of flat plate solar collectors obtained by study the effect of the mass flow rate on fraction load. This study shown that the thermal performance increase gradually by increase the mass flow rate until to reach to the maximum value at mass flow rate 0.02 after that starts decreases. Figure 6.39 shows the variation of fraction load by solar energy values with the mass flow rate values for the three models of flat plate solar collectors. This study obtained for the annually calculation which give us a hence about the mass flow rate by the collector area suitable for the typical design parameter range for the liquid solar heating system. As a results, it is observed that this figure indicates validity of the present solution in this study for fraction load analysis.

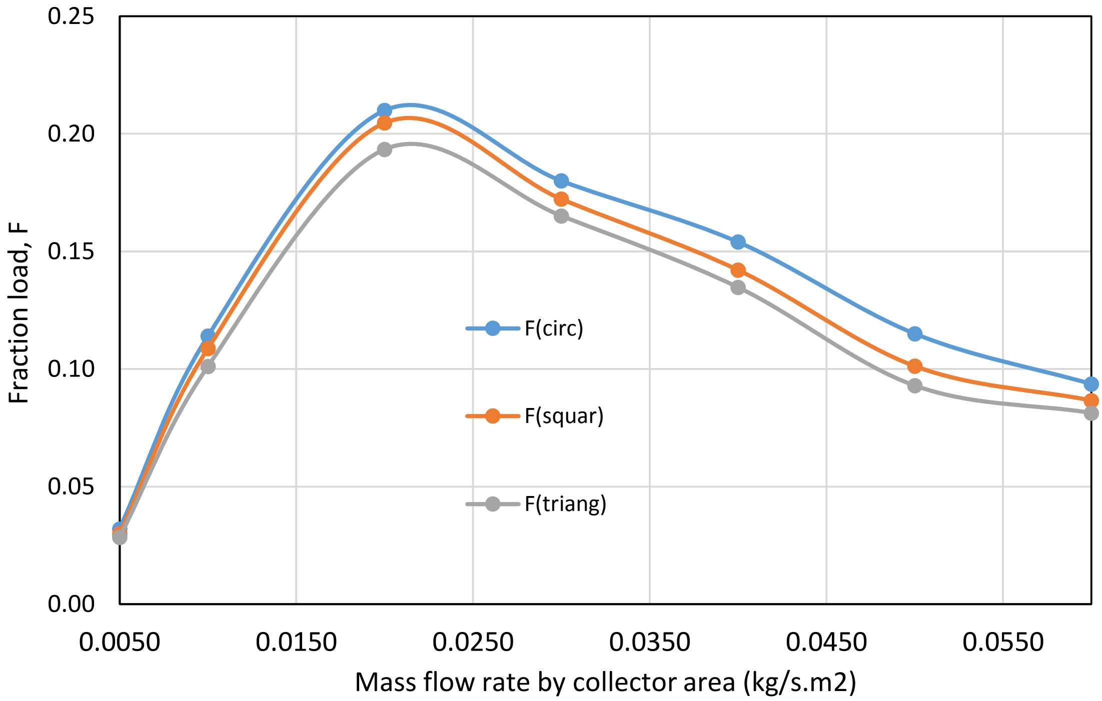

Figure 6.39 Variation of the fraction load values with the values of mass flow rate (kg/s.m^2).

6.5 Results for economical analysis

In order to obtain the circular flat plate solar collector design and the collector area, an economical analysis is required. All of the numerical calculation were realized to obtain economical analysis which is obtained by using the fraction load results. the problem is to determine the size of solar energy system that give the lowest cost combination of the solar energy. In this section we obtained the life cycle savings method of doing economics analyses. This method take into account the time value of money and allow detailed consideration of complete range of costs. The economical analysis based on the life cycle solar savings (LCS) to find the collector size that combination of the solar energy and which provides the highest savings. Now we applied the ideas in this study to illustrate the principles and steps in the life saving analysis the select the optimum design will be based on the solar saving calculation for several collector areas. Figure 6.40 shows the variation of the life cycle solar savings (LCS) with collector area obtained in the present study for annual fraction load. The figure shows that the life cycle solar savings (LCS) values for different collector areas which increase with increase the collector area until reach to maximum value of the life cycle solar savings (LCS) at collector area was $4m^2$ after that starts decreases this the reason shows the validity of the solution method presented in this study. The second reason the value was calculated in P2 C_A/P1 C_{F1} L equation the same value was calculated from the slope equation then that indicates the validity of the solution in this study where the value was calculated from P2 C_A/P1 C_{F1} L was 0.0279 and the value obtained from the slope equation 0.0281 where the collector area Ac is about 4 m^2 then the maximum value of the life cycle solar savings (LCS) at collector area was $4m^2$. As a results, it is observed that this figure indicates validity of the present solution in this study for the economics analysis. The below figure represent the effect of the collector area on the life cycle solar saving. At the same value was calculated the fraction load we obtained the maximum value of the life cycle solar savings (LCS) at collector area was $4m^2$.

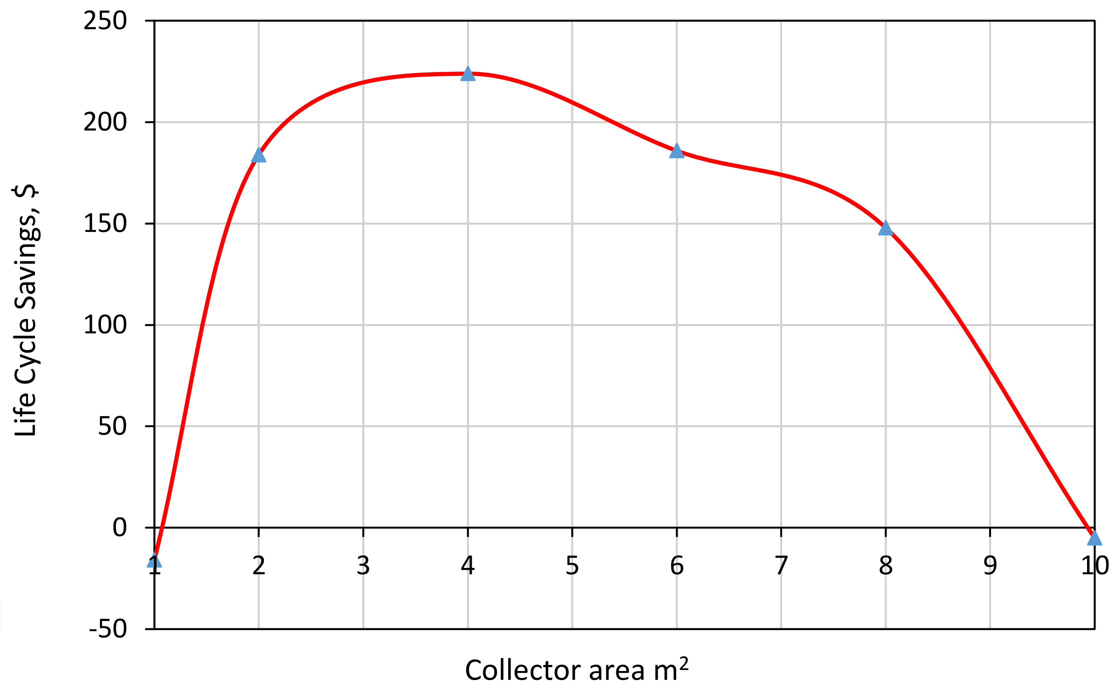

Figure 6.40 Variation of the life cycle savings values with the values of the collector area.

The table below shown the values of the collector area and life cycle solar savings (LCS) and the values of the fraction load by solar energy.

Table 6.2 life cycle savings and collector area.

Collector area(m^2)	LCS($)	FL
1	-16	0.0325
2	184	0.0964
4	224	0.16
6	186	0.2184
8	148	0.264
10	-5	0.292

6.6 Annual fraction load with diameter of tubes

In this section, the calculation of the fraction load by the solar energy for the trapezoidal, ellipsoidal, circular models of flat plate solar collectors obtained by study the effect of the tube diameter on fraction load. This study shown that the thermal performance increase gradually by increase the tube diameter up to reach to the maximum value about 0.15m. Figure 6.41 shows the variation of fraction load by solar energy values with the tube diameter values for the flat plate solar collectors. This study obtained for the annually calculation which give us a hence about the tube diameter by the collector size suitable for the typical design parameter range for the liquid solar heating system.

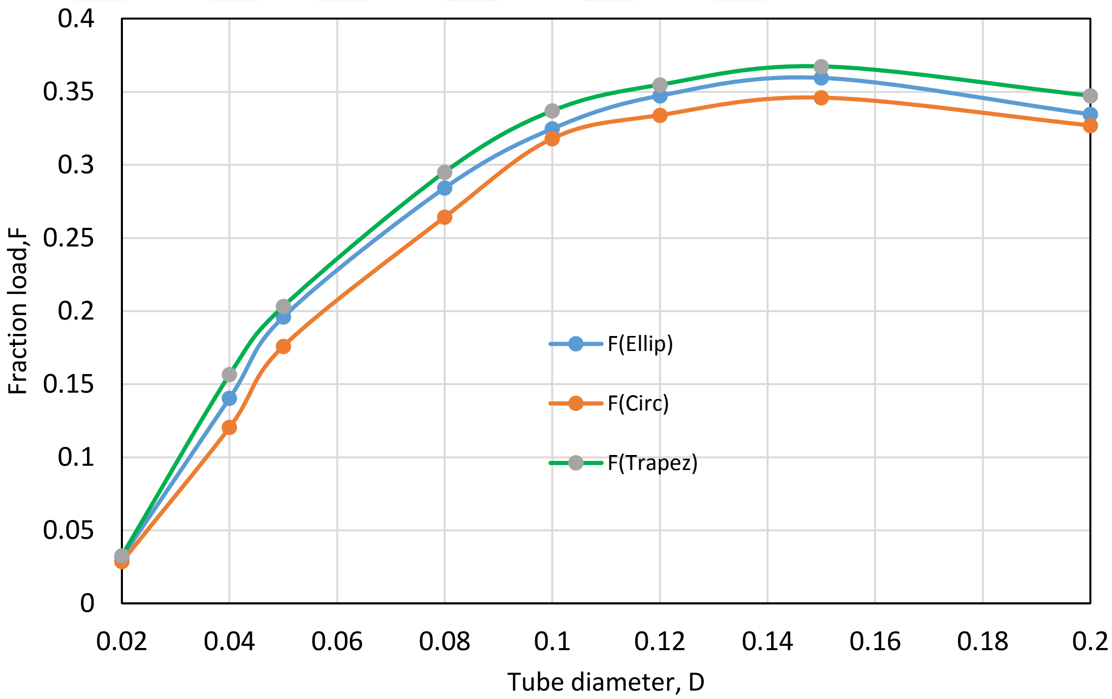

Figure 6.41 Variation of the fraction load values with the values of tube diameter (m)

6.7 Factors of the collector with diameter of tubes

In this section, the calculation of factors of the collector (specifically, heat removal factor, collector efficiency factor, and fin efficiency factor) for the five model of flat plate solar collectors obtained by study the effect of the tube diameter on factors of the collector. This study shown that fin efficiency decrease gradually by increase the tube diameter. Figures 6.42 and 6.43 show the variation of factors of the collector values with the tube diameter values for the flat plate solar collectors.

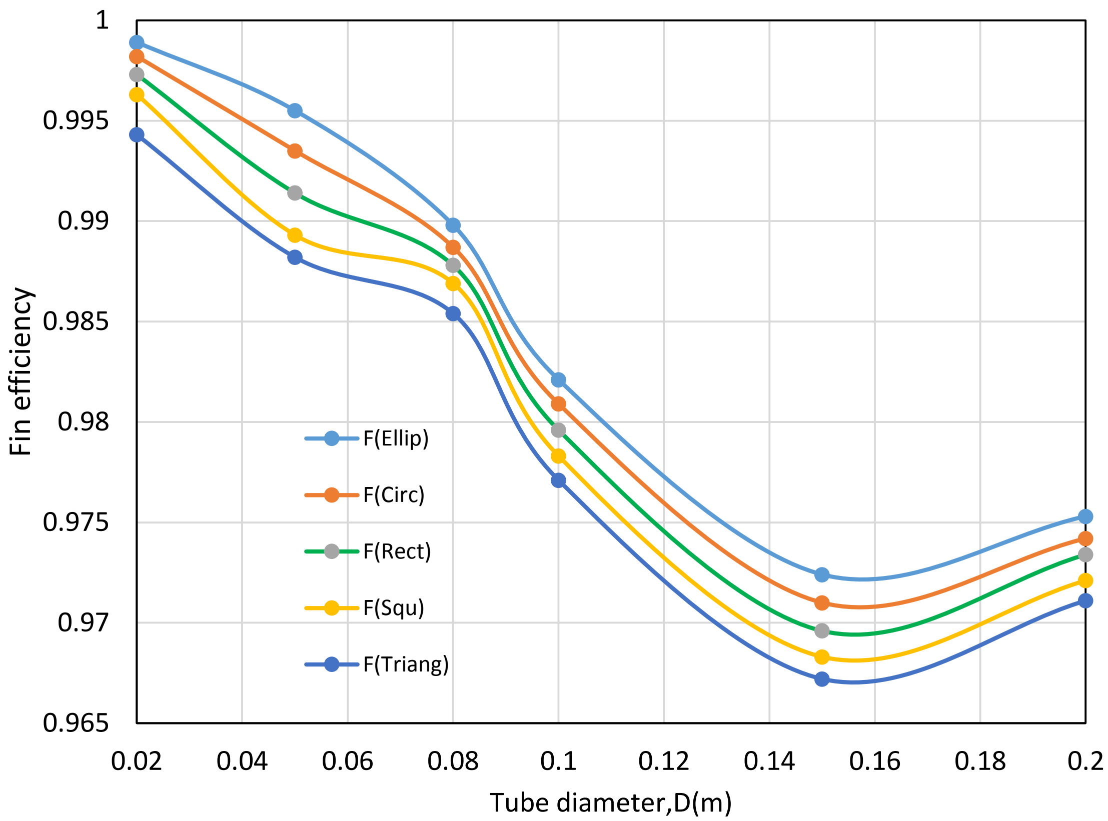

Figure 6.42 Variation of the factors of the collector values with the values of tube diameter (m)

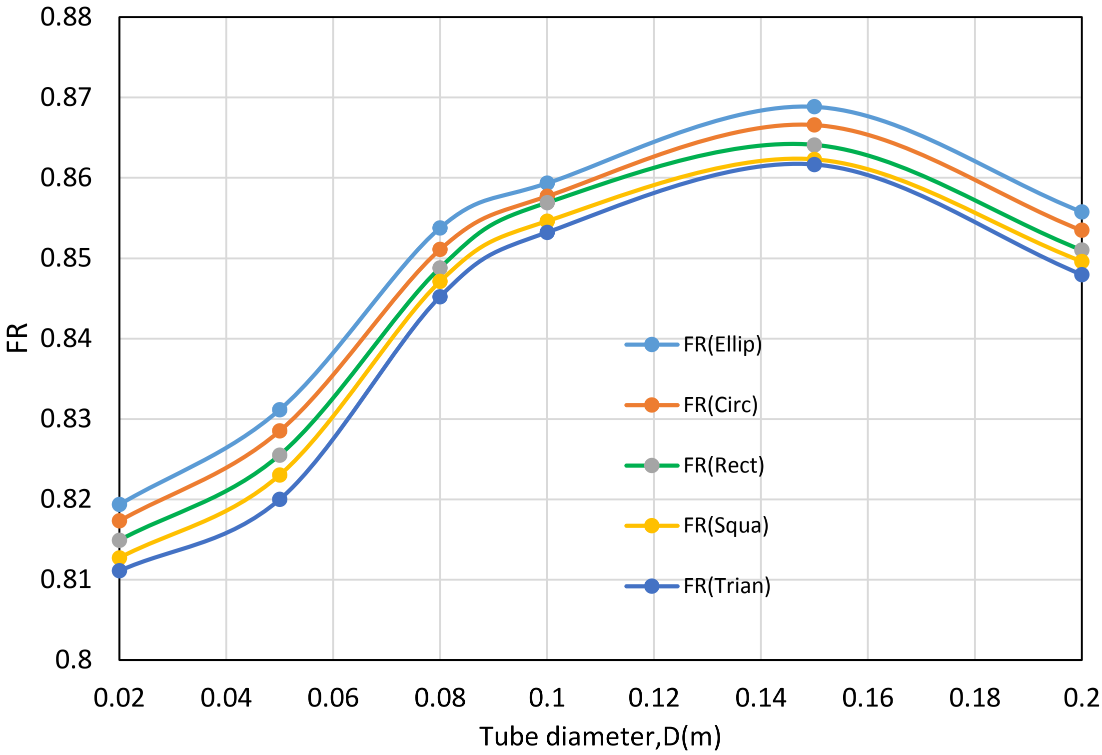

Figure 6.43 Variation of the factors of the collector values with the values of tube diameter (m)

6.8 Comparative study for the ellipsoidal and circular tubes of collectors

From this study it is concluded that elliptical tube gives the maximum outlet temperature of water comparison with circular and other geometries. This shows that elliptical tube is beneficial in future for domestic purpose. The ANSYS simulation results characterized fit the present ones. Then the results obtained by circular compared with best result obtained elliptical. The curves are plotted to indicate simulated outlet temperatures of circular pipe and elliptical pipe versus time. It seems that the difference between simulated outlet temperature of circular pipe and elliptical pipe for different times is almost 4.2℃ [25]. Figure 6.44 and 6.45 show Variation of outlet temperature with time for ellipsoidal and circular models of collectors.

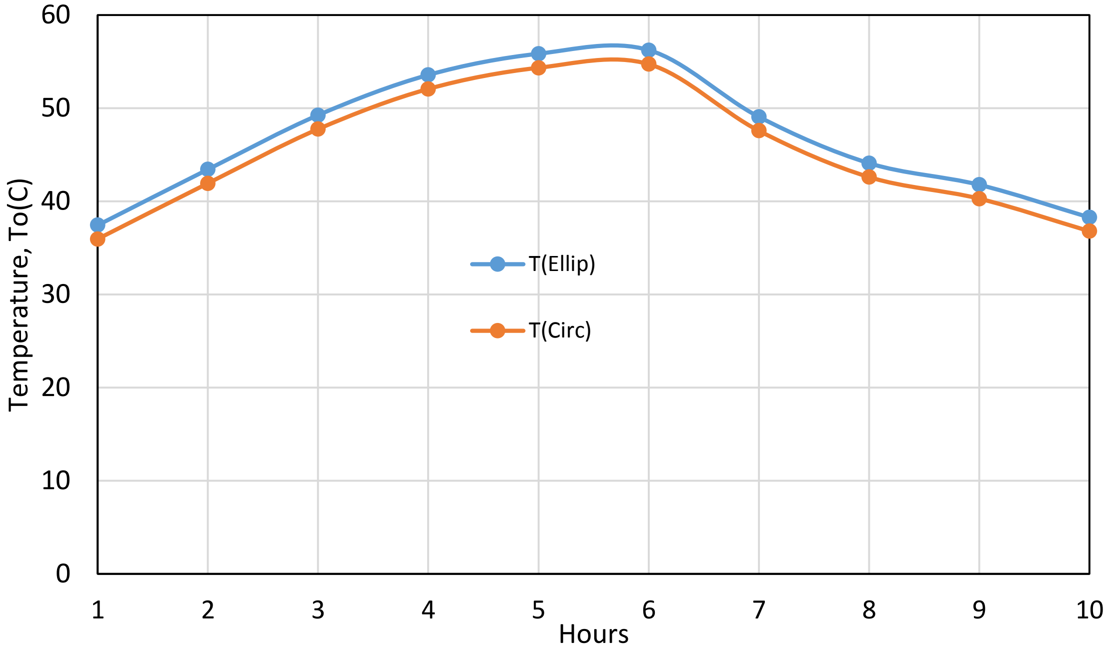

Figure 6.44 Variation of outlet temperature with time for ellipsoidal and circular models of collectors.

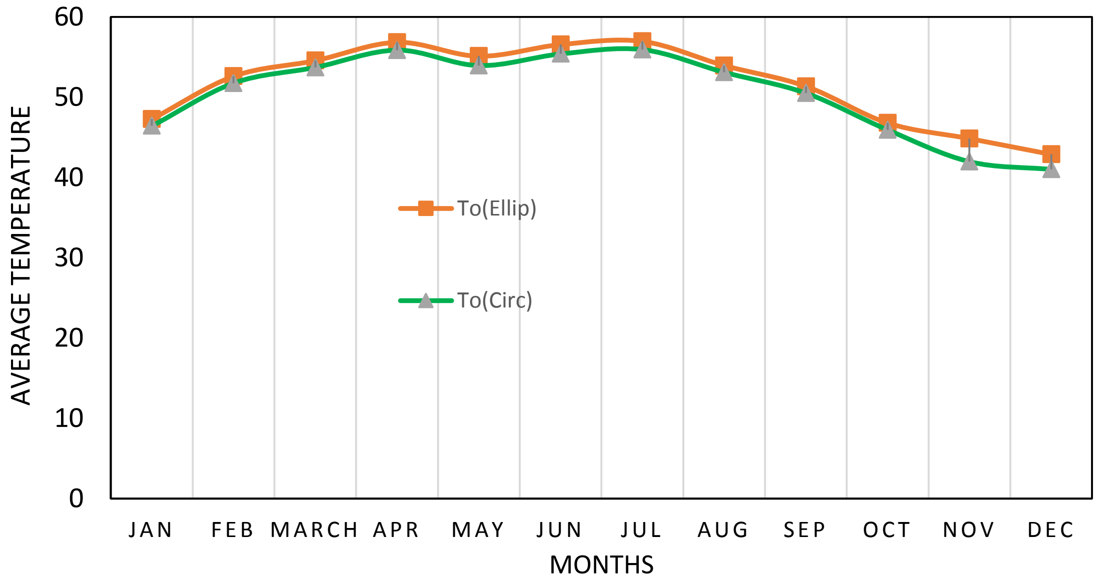

Figure 6.45 Variation of outlet temperature with months for ellipsoidal and circular models of collectors.

6.9 Validation of the theoretical study for this thesis

There is an important question: how reliable is this theoretical study? In order to give a correct answer to this question, it is necessary to check the validation of the solution obtained for all calculation in this thesis to object the enhancement of flat plate solar storage collector by optimization diameter and geometry based on the multi reasons that gave in the Duffie, J.A. and Beckman handbook [24]. Therefore, validation of the study will be checked in this section. The annual fraction load values for different collector areas which increase with increase the collector area this first reason shows the validity of the solution method presented in this study. The second reason the value was calculated in P2 C_A/P1 C_{F1} L equation the same value was calculated from the slope equation then that indicates the validity of the solution in this study where the value was calculated from P2 C_A/P1 C_{F1} L was 0.0279 and the value obtained from the slope equation 0.0281 where the collector area Ac is about 4 $m^2$and the maximum value of the life cycle solar savings (LCS) at collector area was 4m^2. Finally, the f-chart values taken from f-chart method and calculated f-calculation method for the circular flat plate solar collector are closer to each other.

CHAPTER 7

CONCLUSIONS AND RECOMMENDATIONS FOR FUTURE WORK

7.1 Conclusions

The following conclusions can be drawn from the present work:

1. This investigation on three geometries trapezoidal, ellipsoidal, circular, square and triangle models of flat plate solar collector gave us hence to select which type it is optimum so the trapezoidal model which placed into the flat plate solar collector had a positive effect on efficiency of collector.

2. In the solar collector the variation of water temperature difference and collector efficiency with time between outlet and inlet was higher in trapezoidal, ellipsoidal, circular, square and triangle models respectively.

3. This enhancement must give us an experimental fact of the possibility to use flat plate solar storage collector in Iraq-Baghdad to heat water for many application.

4. Flat-plate solar storage collector make important contributions to the energy supplies in IRAQ, because there is plenty of space and sunlight available there. It is very important for the future, because our resources are limited, except our sun.

5. Best model in between five geometry is trapezoidal, w=D is the best conditions.

6. Dopt=0.15m for the best cross section, this may be used as storage collector without tank for lower cost solar energy application.

7.2 Recommendations for Future Work

1. Studying other geometries of solar water heater like a double-pass solar collector to obtain a high outlet temperature and to minimize the heat losses.

2. Studying effect of inserting porous media inside the channels and the impact of these materials on the performance of solar collector.

3. Studying the performance of solar water collector using an auxiliary power source in the case of lack of incident solar energy because of the clouds or the absence of the sun.

4. Use of insulated storage tank for the collector to minimize the approximation error in the ambient-tank free convection coefficient.

REFERENCES

[1] Zhao, D. L., Li, Y., Dai, Y. J., & Wang, R. Z. (2011). Optimal study of a solar air heating system with pebble bed energy storage. *Energy conversion and management*, ***52*(6)**, 2392-2400.

[2] NASA "Surface Meteorology and Solar Energy –Available Table"

Atmospheric Science Data Center, 2008.

[4] Hassan, M. M. (2000). Framework for evaluation of active solar collection systems.

[5] Jones,G.,ECOShift Environmental Blog, http://www.ecoshift.ca/, November (2006).

[6] Hasan, A. (1997). Thermosyphon solar water heaters: effect of storage tank volume and configuration on efficiency. *Energy conversion and management*, ***38*(9)**, 847-854.

[7] Agbo, S. N. (2006). Effect of hot water withdrawal rate on a mean system temperature of a thermosyphon solar water heater. *The Pacific Journal of Sci. and Technology*, **(7)**, 33-42.

[8] Chiou, J. P. (1982). The effect of nonuniform fluid flow distribution on the thermal performance of solar collector. *Solar Energy*, **29(6),** 487-502.

[9] Shariah, A. M., Rousan, A., Rousan, K. K., & Ahmad, A. A. (1999). Effect of thermal conductivity of absorber plate on the performance of a solar water heater. *Applied Thermal Engineering*, **19(7),** 733-741.

[10] Zerrouki, A., Boumedien, A., & Bouhadef, K. (2002). The natural circulation solar water heater model with linear temperature distribution. *Renewable Energy*, **26(4),** 549-559.

[11] Kundu, B. (2008). Performance and optimum design analysis of an absorber plate fin using recto-trapezoidal profile. *Solar Energy*, **82(1),** 22-32.

[12] Kalogirou, S. A. (2014). Flat-plate collector construction and system configuration to optimize the thermosiphonic effect. *Renewable energy*, **67,** 202-206.

[13] Abd-al Zahra, H. A. A., & Joudi, H. A. (1984). An experimental investigation into the performance of a domestic thermosyphon solar water heater under varying operating conditions. *Energy conversion and management*, **24(3),** 205-214.

[14] Sekhar, Y. R., Sharma, K. V., & Rao, M. B. (2009). Evaluation of heat loss coefficients in solar flat plate collectors. *ARPN journal of engineering and Applied Sciences*, **4(5),** 15-19.

[15] Hobbi, A., & Siddiqui, K. (2009). Experimental study on the effect of heat transfer enhancement devices in flat-plate solar collectors. *International Journal of Heat and Mass Transfer*, **52(19-20),** 4650-4658.

[16] Sutthivirode, K., Namprakai, P., & Roonprasang, N. (2009). A new version of a solar water heating system coupled with a solar water pump. *Applied Energy*, **86(9),** 1423-1430.

[17] Jaisankar, S., Radhakrishnan, T. K., & Sheeba, K. N. (2009). Experimental studies on heat transfer and friction factor characteristics of thermosyphon solar water heater system fitted with spacer at the trailing edge of twisted tapes. *Applied Thermal Engineering*, **29(5-6),** 1224-1231.

[18] Huang, J., Pu, S., Gao, W., & Que, Y. (2010). Experimental investigation on thermal performance of thermosyphon flat-plate solar water heater with a mantle heat exchanger. *Energy*, **35(9),** 3563-3568.

[19] Tang, R., Cheng, Y., Wu, M., Li, Z., & Yu, Y. (2010). Experimental and modeling studies on thermosiphon domestic solar water heaters with flat-plate collectors at clear nights. *Energy Conversion and Management*, **51(12),** 2548-2556.

[20] Hassab, M. A., Sorour, M. M., & Elewa, F. (1987). An optimum performance of flat-type solar air heater with porous absorber. *International journal of energy research,* **11(4),** 479-489.

[21] Chen, W., & Liu, W. (2004). Numerical analysis of heat transfer in a composite wall solar-collector system with a porous absorber. *Applied Energy*, **78(2),** 137-149.

[22] Yousef, B. A. A., & Adam, N. M. (2008). Performance analysis for flat plate collector with and without porous media. *Journal of Energy in Southern Africa*, ***19*(4)**, 32-42.

[23] Chen, C. C., & Huang, P. C. (2012). Numerical study of heat transfer enhancement for a novel flat-plate solar water collector using metal-foam blocks. *International Journal of Heat and Mass Transfer*, **55**(23-24), 6734-6756.

[24] Duffie, J.A. and Beckman, W.A., Solar Engineering and Thermal Process, John Wiley and Sons, New York, (1980).

[25] Shelke, V. G., & Patil, C. V. (2015). Analyze the Effect of Variations in Shape of Tubes for Flat Plate Solar Water Heater. *International Journal of Scientific Engineering and Research*, 118-124.

APPENDIX A

SAMPLE OF COMPUTER PROGRAMING

```
% **Input Data**
I= [hourly solar radiation from sunrise to sunset for whole year (January to
December)];
 % incident radiation
Ta= [hourly ambient temperature from sunrise to sunset for whole year (January to
December)];
  % ambient temp.

A= collector area;
Fsh= Shading coefficient;
Fd= Dust coefficient;
alpha_p=0.95;
TAU=0.88;
cp=4190;
k=0.029 ;
Kb=0.03;Xb=0.05;
w=spacing tube;
siqma=5.67*10^-8;Eg=0.88;Ep=0.95;bita=tilt angle;
Ft=1.02*alpha_p*TAU*Fsh*Fd;
Dh=hydraulic diameter for three type of collector tubes; % hydraulic dia.
mdot=mass flow rate;
L= %plate spacing
v= [hourly wind speed from sunrise to sunset for whole year (January to December)];
%velocity

% Calculations

Ub=Kb/Xb; Ue=(Ke/Xe)*(P*t/A);
hw=5.7+3.8*v;
for i=1:n;
Qab(i)=Ft*I(i)*A;
hrga(i)=Eg*siqma*(Tg(i)+Ta(i))*((Tg(i))^2+(Ta(i))^2);

% radiation heat transfer coeff. from glass to ambiant
hrpg(i)=(siqma*(Tp(i)+Tg(i))*((Tp(i))^2+(Tg(i))^2))/((1/Ep)+(1/Eg)-1);

% radiation heat transfer coeff. from plate to glass

Tm(i)=(Tp(i)+Tg(i))/2;
```

```
Ra(i)=9.81*(Tp(i)-Tg(i))*L^3/(Tm(i)*new*alpha);

aa(i)=1-(1708*cos(bita)/Ra(i));

bb(i)=((Ra(i)*cos(bita)/5830)^(1/3)-1);

Nu(i)=1+1.44*(1-((1708*sin(1.8*bita)^1.6)/(Ra(i)*cos(bita))))*aa(i)+bb(i);

hcpg(i)=Nu(i)*k/L;

Ut(i)=((1/(hcpg(i)+hrpg(i)))+(1/(hw(i)+hrga(i))))^-1;

Ul(i)=Ut(i)+Ub+Ue;

m(i)=(Ul(i)/K delta)^0.5;

F(i)=(tanh(m(i)*(w-Dh)*0.5))/(m(i)*(w-Dh)*0.5);

xx(i)=1/((Dh/w)+(1/(w/(w-Dh)*F(i))));

F_dash(i)=1/(xx(i)+((w*Ul(i))/(3.14*Dh*h(i))));

z(i)=mdot*cp/(A*Ul(i)*F_dash(i));

F_doubldash(i)=z(i)*(1-exp(-1/z(i)));

Fr(i)=F_dash(i)*F_doubldash(i);
S(i)=Ft*I(i);

Qu(i)=Fr(i)*A*(S(i)-(Ul(i)*(Ti(i)-Ta(i))));

Tp(i)=Ti(i)+((Qu(i)*(1-Fr(i)))/(Fr(i)*Ul(i)*A));

Ql(i)=Ul(i)*A*(Tpmean(i)-Ta(i));

To(i)=[Ti(i)+(Qu(i)/(mdot*cp))]-c;

Qi(i)=I(i)*A;

eff(i)=Qu(i)/Qi(i);

Qst(i)=Qi(i)-Qu(i)-Ql(i);

ss(i)=4*Fr(i)*((S(i)*0.0036)-(0.0036*Ul(i)*(Ts-(Ta(i)-c))));


end
% Important Results

Qu
```

```
To
Fr
Qst
eff
Qi
Nu
Ra
h
Qu
Qab
F
F_dash
F_doubldash
Ul
m
hcpg
hrpg
hrga
hw
S
Ft
Ut
Ub
Ql

I= [monthly average daily radiation incident on the collector surface per unit area (J/m2)];
 % incident radiation
Ta=[monthly average ambient temperature (C) ];
 % ambiant temp.
N=[number of days in month];
FR=[average heat removal factor value per month];
 %.
Ul=[ average overall heat loss coefficient values per month];
 % input.
for i=1:12
Lw(i)=water heating load;
X(i)=(FR(i)*Ul(i))*N(i)*86400*(Ac/Lw(i));
XC(i)=(11.6 + 1.8Tw + 3.86Tm - (2.37*Ta(i)));
XX(i)=X(i)*XC(i);
Y(i)= FR(ta) *I(i)*1000000*N(i)*(Ac/Lw(i));
```

```
f(i)=((1.029*Y(i))-(0.065*XX(i))-
(0.245*Y(i)*Y(i))+(0.0018*XX(i)*XX(i))+(0.0215*Y(i)*Y(i)*Y(i)));
fll(i)=f(i)*Lw(i)*0.000000001;
F = Σ f * Lw(i) / Σ Lw(i);
dF/dA=P2 C_A/P1 C_F1 L
LCS=P1 C_F1 L F-P2 (C_A A_C+C_E)


end
% Important Results


X
XC
XX
Y
fll
Lw
L
F
f
LCS
dF/dA
```

APPENDIX B

TABLES

The table B.1 shows calculate annually fraction load by solar energy for collector area 1 m^2.

months	L	f*L	X	Y	f
Jan	2.922525	0.035964	0.181086	0.023471	0.012306
Feb	2.733975	0.059714	0.16445	0.031807	0.021842
March	2.922525	0.08889	0.148486	0.039265	0.030415
Apr	2.82825	0.100698	0.119525	0.042556	0.035604
May	2.922525	0.13254	0.101891	0.05111	0.045351
Jun	2.82825	0.156776	0.078572	0.059665	0.055432
Jul	2.922525	0.151145	0.068115	0.055278	0.051717
Aug	2.922525	0.14377	0.073118	0.053085	0.049194
Sep	2.82825	0.110194	0.088094	0.043872	0.038962
Oct	2.922525	0.072003	0.11421	0.031368	0.024637
Nov	2.82825	0.041289	0.145484	0.023471	0.014599
Dec	2.922525	0.031232	0.161134	0.02062	0.010687
	F=0.0325				

The table B.2 shows calculate annually fraction load by solar energy for collector area 2 m^2.

months	L	f*L	X	Y	f
Jan	2.922525	0.071489	0.362172	0.046943	0.024461
Feb	2.733975	0.118351	0.328899	0.063614	0.043289
March	2.922525	0.175827	0.296972	0.07853	0.060163
Apr	2.82825	0.199059	0.239049	0.085111	0.070382
May	2.922525	0.2615	0.203781	0.102221	0.089477
Jun	2.82825	0.308758	0.157145	0.119331	0.109169
Jul	2.922525	0.298027	0.136229	0.110557	0.101976
Aug	2.922525	0.283618	0.146236	0.106169	0.097046
Sep	2.82825	0.217831	0.176188	0.087743	0.07702
Oct	2.922525	0.142746	0.228421	0.062736	0.048843
Nov	2.82825	0.082036	0.290968	0.046943	0.029006
Dec	2.922525	0.062132	0.322269	0.041239	0.02126
	F=0.064				

The table B.3 shows calculate annually fraction load by solar energy for collector area 4 m^2.

months	L	f*L	X	Y	f
Jan	2.922525	0.141241	0.724345	0.093885	0.048328
Feb	2.733975	0.232437	0.657798	0.127228	0.085018
March	2.922525	0.343933	0.593944	0.157061	0.117684
Apr	2.82825	0.388886	0.478098	0.170222	0.137501
May	2.922525	0.508875	0.407563	0.204442	0.174122
Jun	2.82825	0.598653	0.314289	0.238662	0.211669
Jul	2.922525	0.579254	0.272458	0.221113	0.198203
Aug	2.922525	0.55177	0.292473	0.212339	0.188799
Sep	2.82825	0.425556	0.352376	0.175487	0.150466
Oct	2.922525	0.280498	0.456842	0.125473	0.095978
Nov	2.82825	0.161917	0.581935	0.093885	0.05725
Dec	2.922525	0.122947	0.644537	0.082479	0.042069
	F=0.126				

The table B.4 shows calculate annually fraction load by solar energy for collector area 6 m^2.

months	L	f*L	X	Y	f
Jan	2.922525	0.209295	1.086517	0.140828	0.071614
Feb	2.733975	0.342347	0.986698	0.190842	0.12522
March	2.922525	0.504501	0.890916	0.235591	0.172625
Apr	2.82825	0.569706	0.717148	0.255333	0.201434
May	2.922525	0.742529	0.611344	0.306663	0.254071
Jun	2.82825	0.870306	0.471434	0.357993	0.307719
Jul	2.922525	0.844193	0.408687	0.33167	0.288857
Aug	2.922525	0.804908	0.438709	0.318508	0.275415
Sep	2.82825	0.623419	0.528564	0.26323	0.220426
Oct	2.922525	0.413348	0.685263	0.188209	0.141435
Nov	2.82825	0.239683	0.872903	0.140828	0.084746
Dec	2.922525	0.182473	0.966806	0.123718	0.062437
	F=0.184				

The table B.5 shows calculate annually fraction load by solar energy for collector area 8 m^2.

months	L	f*L	X	Y	f
Jan	2.922525	0.275691	1.44869	0.187771	0.094333
Feb	2.733975	0.448174	1.315597	0.254456	0.163927
March	2.922525	0.657713	1.187887	0.314121	0.22505
Apr	2.82825	0.741743	0.956197	0.340444	0.262262
May	2.922525	0.962865	0.815125	0.408884	0.329463
Jun	2.82825	1.124335	0.628578	0.477324	0.397537
Jul	2.922525	1.093351	0.544916	0.442226	0.374112
Aug	2.922525	1.043483	0.584946	0.424678	0.357048
Sep	2.82825	0.811669	0.704753	0.350973	0.286986
Oct	2.922525	0.541391	0.913684	0.250946	0.185248
Nov	2.82825	0.315369	1.163871	0.187771	0.111507
Dec	2.922525	0.240735	1.289074	0.164957	0.082372
	F=0.24				

The table B.6 shows calculate annually fraction load by solar energy for collector area 10 m^2.

months	L	f*L	X	Y	f
Jan	2.922525	0.340467	1.810862	0.234713	0.116497
Feb	2.733975	0.550007	1.644496	0.318069	0.201175
March	2.922525	0.803752	1.484859	0.392651	0.27502
Apr	2.82825	0.905223	1.195246	0.425555	0.320065
May	2.922525	1.170285	1.018906	0.511105	0.400436
Jun	2.82825	1.361362	0.785723	0.596654	0.481344
Jul	2.922525	1.32724	0.681146	0.552783	0.454141
Aug	2.922525	1.267945	0.731182	0.530847	0.433853
Sep	2.82825	0.990552	0.880941	0.438717	0.350235
Oct	2.922525	0.664719	1.142104	0.313682	0.227447
Nov	2.82825	0.389015	1.454839	0.234713	0.137546
Dec	2.922525	0.29776	1.611343	0.206197	0.101885
	F=0.2926				